



**UNIVERSITY OF THE PELOPONNESE**

---

**Mavropoulou Maria-Eleni**

**(R.N. 1012201502006)**

**DIPLOMA THESIS:**

A technological analysis of Mycenaean wall-paintings from Iklaina,  
Peloponnese.

---

**SUPERVISING COMMITTEE:**

- Associate Researcher Hariklia Brecolaki, (National Hellenic Research Foundation)
- Associate Professor Nikos Zacharias, (University of the Peloponnese)

**EXAMINATION COMMITTEE:**

- Associate Researcher Hariklia Brecolaki, (National Hellenic Research Foundation)
- Associate Professor Nikos Zacharias, (University of the Peloponnese)
- Professor Michael Basil Cosmopoulos, (University of Missouri, St Louis)

**KALAMATA, JANUARY 2017**



## **Acknowledgements**

I would like to express my gratitude to Mrs. Maria Kylafi, archaeologist of the Ephorate of Antiquities of Messenia, who despite her tight schedule managed to find time to handle the permission quickly so as to acquire the samples. A very special thank you to Ms Eleni Palamara, PhD candidate in the University of the Peloponnese, and Mrs. Sylia Valadou for their patience and guidance during the sessions in the Laboratory of Archaeometry and to my professors: Mrs Hariclia Brecoulaki, Assistant Researcher at National Hellenic Research Foundation for giving me the chance to be engaged with such an archaeological material, Associate Professor Mr. Nikolaos Zacharias for his trust in me and Professor Mr. Michael Basil Cosmopoulos for allowing me to research material from the Iklaina Archaeological Project and his tour of the excavation site.

## Table of Contents

Acknowledgements.....	3
Table of Contents.....	4
Table of Tables .....	5
Abstract.....	7
Introduction.....	7
1.The Samples.....	11
2.The Mortars.....	11
3. The Pigments .....	20
3.1 Blue.....	21
3.2 Red.....	30
3.3 Pink.....	34
3.4 Yellow .....	36
3.5 Black.....	37
4.Discussion.....	48
5.Conclusion .....	50
Appendix.....	52
References.....	70

## Table of Tables

Table 1: Major element oxides in *wt%* normalised to 100% as detected in the XRF.

Table 2: Table of the trace elements of mortars detected in XRF. Values are shown in *ppm*. (A complete table can be found in the appendix: Table 2)

Table 3: Table showing the mean values in *%wt* and standard deviations of each sample as measured in SEM.

Table 4: Mean values of CaO, Al<sub>2</sub>O<sub>3</sub> SiO<sub>2</sub> in *%wt* as measured in the SEM and the ratio of Al<sub>2</sub>O<sub>3</sub>/SiO<sub>2</sub>. BDL stands for Below Detection Limit, while \* represents the lack of data.

Table 5: Chemical analysis of s01 in SEM. Mean values and standard deviation. All results are shown in compound% and are normalised.

Table 6: Chemical analysis of s04 dark blue in SEM. Mean values and standard deviation. All results are shown in compound% and are normalised.

Table 7: Chemical analysis of s05 in SEM. Mean values and standard deviation. All results are shown in compound% and are normalised.

Table 8: Chemical analysis of s10 in SEM. Mean values and standard deviation. All results are shown in compound% and are normalised.

Table 9: Chemical analysis of s11 in SEM. Mean values and standard deviation. All results are shown in compound% and are normalised.

Table 10: Chemical analysis of s02-blue in SEM. Mean values and standard deviation. All results are shown in compound% and are normalised.

Table 11: Chemical analysis of s07 in SEM. Mean values and standard deviation. All results are shown in compound% and are normalised.

Table 12: Chemical analysis of s06 in SEM. Mean values and standard deviation. All results are shown in compound% and are normalised.

Table 13: Chemical analysis of s02 red in SEM. Mean values and standard deviation. All results are shown in compound% and are normalised.

Table 14: Chemical analysis of s08 in SEM. Mean values and standard deviation. All results are shown in compound% and are normalised.

Table 15: Chemical analysis of s13 in SEM. Mean values and standard deviation. All results are shown in compound% and are normalised.

Table 16: Chemical analysis of s03 in SEM. Mean values and standard deviation. All results are shown in compound% and are normalised.

Table 17: Chemical analysis of s14 in SEM. Mean values and standard deviation. All results are shown in compound% and are normalised.

Table 18: Chemical analysis of s09 in SEM. Mean values and standard deviation. All results are shown in compound% and are normalised.

Table 19: Chemical analysis of s04 black in SEM. Mean values and standard deviation. All results are shown in compound% and are normalised.

Table 20: Chemical analysis of s12 in SEM. Mean values and standard deviation. All results are shown in compound% and are normalised.

Table 21: Chemical analysis of s15 in SEM. Mean values and standard deviation. All results are shown in compound% and are normalised.

Table 22: Chemical analysis of s15 in SEM. Mean values and standard deviation. All results are shown in compound% and are normalised.

Table 23: Summative table of the sample pigments along with their SEM images.

Table 24: Chemical analysis of s01 in BSE. All results are shown in compound% and are normalised.

Table 25: Chemical analysis of s01 in BSE. All results are shown in compound% and are normalised.

Table 26: Chemical analysis of the areas of s02 red as outlined in fig. 34.

Table 27: Chemical analysis of the s12 areas outlined in fig. 36.

### **Tables in the Appendix**

Table 1: Photos of all the samples as received.

Table 2: Trace elements of mortars as detected in XRF. Values shown in ppm.

Table 3: Complete results of mortar and pigment analysis of the samples in XRF and in SEM. Major element oxides in wt% normalised to 100% as detected in the XRF, analysis results in SEM are shown in compound %wt and are normalised.

## Abstract

This study is about the examination of Mycenaean wall painting fragments from Iklaina in the vicinity of Pylos. It aims to provide an analysis of the mortars, check the chemical composition of the pigments and their layers. For this purpose analytical techniques were employed. The samples were examined in a LED microscope, in a micro X-ray fluorescence spectrometer and in a scanning electron microscope paired with an energy dispersive spectrometer. The results were analysed qualitatively and quantitatively as necessary, by analysing spectra, calculating mean values and the standard deviation and creating biplots.

In the following chapters are presented some archaeological information about the site where the samples come from, a presentation of the instrumentation used and its limitations, followed by chapters on the mortars and the pigments. The final chapter deals with what has been found, what remains inconclusive, and how can the research be extended by satisfyingly answering these questions.

## Introduction

The scope of this research is the technological analysis of fresco fragments from the site of Iklaina: Traganes (fig. 1). The site was identified by R. Hope and J. Bennet but it was S. Marinatos that did some initial investigation back in the 1950s (Marinatos, 1954). Left unexplored for several decades thereafter, it was in 1999 that the Iklaina Archaeological Project was developed and launched. The project consisted of two phases. The first included an intensive archaeological and geophysical survey of the lands nearby (1999-2006), while the second involved a full scale excavation spanning through several years (2006 to this day (Cosmopoulos, 2015a).



**Figure 1: Aerial photograph of the excavation site in Iklaina as taken by the official website of the Iklaina Archaeological Project (<http://www.iklaina.org/>)**

The excavation has yielded a large surface covered with architectural features (Cyclopean Terrace Building, houses, workshops, roads, open terraces, water pipes, pottery, fresco fragments etc)<sup>1</sup>. From the findings the site can be dated from Middle Helladic (MH) or early Late Helladic (LH) period to the end of the Mycenaean period (Cosmopoulos, 2015a). Of the most impressive structures is the Cyclopean terrace of rectangular shape with two series of serrations similar to the ones found in the terraces in Pylos, Gla and Tyrins. The use of the terrace was to support the flat extension of the southern plateau. On the terrace was a possible two-floor building as indicated by a few uncovered stairs. To the east of the terrace extends a paved court. Access to the court and the rooms to the south was feasible by an as well paved ramp. (Cosmopoulos, 2012) The three rooms to the south were part of another building (building T) probably used for as warehouses judging by their size. Inside was found a large number of fresco fragments scattered in all three places probably originating by an upper floor (Cosmopoulos, 2013) dating from LHIIB-LHIIIA1 (Cosmopoulos, 2015a).

Some of the fresco fragments were conjoined and had representations of a rowing ship and a woman in profile. These fragments were studied and about 1/3 of them had visible painted decoration. The mortars varied in thickness and layers, where in most cases there is a thin layer of 2-3mm for smoothing purposes. In a few fragments traces of the tools can be observed. The best preserved of them usually have two layers of thick mortar (1-2cm) and are with better cohesion and less fragility than the thinner ones. The colours seem to be chemically unaltered since the Mycenaean era, with the exception of an unusual green colour which is probably a chemical degradation of Egyptian blue. The rest of the palette consists of the usual earthly colours, carbon black, calcite and Egyptian blue in several different hues. The red pigments are less infused into the underlying colour with obvious signs of peeling (Cosmopoulos, 2015b).

A small number of fifteen fresco fragments were provided to be technologically analyzed in order to understand the creation process of both the mortars and the pigments applied. The samples were examined under a LED microscope, in a portable micro X-ray fluorescence spectrometer (micro-XRF) and in Scanning Electron Microscope paired with an Energy Dispersive Spectrometer (SEM/EDS) all available in the Laboratory of Archaeometry of the University of the Peloponnese. The same instrumentation has been used for other research done in the Laboratory of Archaeometry as is 'Portable XRF for Use in

---

<sup>1</sup> Analytical presentations of the findings have been published in the *Annual Reports of the Athens Archaeological Society (Εργον της εν Αθήναις Αρχαιολογικής Εταιρείας)*, 2006, 2008, 2009, 2010, 2011, 2012.



Archaeology' by I. Liritzis, N. Zacharias (2010) regarding the XRF and 'Analytical and technological examination of glass tesserae from Hagia Sophia' by A. Moropoulou et al (2016) for the SEM-EDS.

For the LED microscopic analysis the FOM i-scope of Moritex was used and all the samples were examined under x10 and x50 magnification. The micro-XRF used was Bruker Tracer III-SD with a beam size 3x4mm. Regarding the mortars two kinds of settings were applied for thorough results. Specifically, for the light elements with  $Z < 26$  a vacuum pump with no filter was applied, while the beam was of 15kV and 24 $\mu$ A that target each sample for 120secs. To detect heavier elements with  $Z > 26$  a filter of Al-Ti was inserted while the accelerating voltage of 40kV and 12 $\mu$ A and the time considered appropriate was again 120secs. The latter settings were used to qualitatively detect the elements with  $Z \geq 22$  for the pigments as well. No sample standards were taken.

The SEM was a model of JEOL (JSM-6510LV) coupled with an EDS by Oxford Instruments. The program software for the quantifications was INCA. The accelerating voltage was 20kV with 40 spot size. The acquisition time was different for each type of material. For the mortars 120secs was suitable and for the pigments only 90secs to avoid destruction of the surface.

All the samples were examined without any prior cleaning or interference. Some of them were afterwards molded in epoxy resin Caldofix-2 for further investigation in the SEM-EDS. A series of silicon carbide grinding foils<sup>2</sup> and four polishing cloths<sup>3</sup> were used consecutively in the polishing device of Struers, Labopol-2. The acquisition time of the cross sectioned samples was 60secs.

From the XRF analysis a series of spectra were acquired providing the detectable elements. Concerning the mortars, the elements were quantitatively analyzed. The values of the major elements were noted as oxides in wt% and normalized to 100%. The trace elements were noted in ppm. Both mortars and pigments were examined in the SEM-EDS. A fresh cut of the mortar sides was considered appropriate when heavily crusted with soil. During the sessions a total of three spectra was considered representative for the bulk analysis of each sample. The final results were then processed to provide a mean value and its standard deviation for each element detected. Then these were combined in a biplot to ascertain the

---

<sup>2</sup> Dimensions: Grit #180, #320, #800, #1200, #2000, #4000.

<sup>3</sup> Sizes: 6 $\mu$ m, 3 $\mu$ m, 1 $\mu$ m and 0.4 $\mu$ m.

purity of the plaster and how similar are the samples. Sometimes a spot analysis was also required while images of several magnifications were taken to better understand the topography of the samples.

All the data were then examined for each sample separately in order to reach to conclusions. In the following chapters is presented an overview and initial description of the samples. The analysis of the mortars and the pigments is presented in different chapters while everything is then discussed.

## 1. The Samples

A total of fifteen samples were provided. They were of irregular shaping or at other times roughly rectangular or trapezoid. Their size was of about 1,5x2cm, while the thickness of the mortar substrate differed variably <1- 1,5cm. All of them had their surfaces covered with crusted soil (both in mortar and pigment sides) and at times the colour was scraped off. The mortars were quite soft, easy to break even by hand. Sample no 6 was consisted only of grains of mortar and pigment. Most samples were monochromatic. However, sample 02 was distinctly consisted of two pigments coloured blue and red, sample 04 of black and blue while samples 12 and 15 were considered having layers of two different colours. An overview of all the samples with images is provided in Table 1 of the appendix.

## 2. The Mortars

Plaster has been used in architecture for structural purposes (mud plaster) and later on for the creation of a smooth surface suitable for decorative painting. At first simple lime plasters were used but then there was a technological advance, the creation of high purity lime plaster. (Morgan 2005, 203) V. Perdikatsis shows the presence of lime consisting mainly of calcite ( $\text{CaCO}_3$ ) with some quartz ( $\text{SiO}_2$ ) impurities. The impurities, organic and inorganic material (quartzitic sand, crushed ceramics or even straw), operated as fillers. The feature of interest is that the calcite can be distinguished in two generations. Those are the primary and secondary calcites respectively. The grain size of the two differs since the first is up to  $100\mu\text{m}$  and the latter up to  $10\mu\text{m}$ . The secondary calcite, which is in fact very fine lime material, shows that the plaster fragments were mixed with slake lime  $\text{Ca}(\text{OH})_2$ .<sup>4</sup> During the process of drying the slaked lime is turned into what is called secondary calcite, with the aid of the atmospheric  $\text{CO}_2$ . This plaster would be highly calcareous high in purity. However, calcareous plaster without fillings is bound to crack. In many cases, a thin layer of fine lime was observed between the main plaster and the pigment layer, showing that it was applied before painting and served as a protective topcoat. (Perdikatsis 1998; Morgan 2005, 208)

All the samples were firstly observed with the LED microscope without any prior preparation. In most cases the samples were heavily crusted with soil; however some traits of

---

<sup>4</sup> Heating calcites in a temperature over  $850^\circ\text{C}$  creates  $\text{CaO}$ . Addition of water reacts in transforming it to slake lime  $\text{Ca}(\text{OH})_2$ . (Perdikatsis 1993)

the plaster could be discerned. The plaster despite its weathered sides seems rather homogeneous with crackings, pores and some inclusions. Some colour diffusion is also considered possible, while in some samples there are different strata with the lower being coarse and the upper closer to the pigment finer.



Figure 2: Sample 3, LED photo magnification x10. Homogeneous mortar with inclusions.



Figure 3: Sample 10, magnification x50. Plenty of pores discernible.

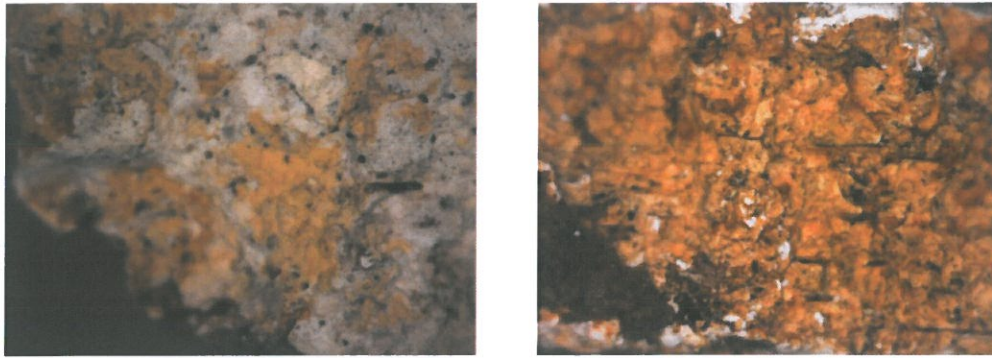


Figure 4: Left: Sample 04, photo magnification x50. Plenty of pores in the mortar's surface. Right: Sample 09, photo magnification x50. Horizontal marks probably left by straw or tool marks.



Figure 5: Sample 10, LED magnification x10. Probable fine thin layer below the pigment.

The next step of investigation was a chemical analysis by means of XRF. Concerning the mortars, it was possible to get quantification results since the thickness was enough to give credibility. In some samples<sup>5</sup> fresh cuts were made to eliminate any alteration by the crusted soil and weathering, compare with the previous measurement or find clear mortar where it was not visible at all. Sample 06 was not examined at all because of its very small grains. The Table 1 below gives the quantified results of the major element oxides in wt%, normalized to 100%

---

<sup>5</sup> Samples: 02, 03, 05, 07, 08, 09, 11, 12, 14, 15.

Samples	Na <sub>2</sub> O	MgO	Al <sub>2</sub> O <sub>3</sub>	SiO <sub>2</sub>	SO <sub>3</sub>	K <sub>2</sub> O	CaO	FeO	SUM
01	1.434	0.792	12.637	38.177	0.585	1.413	44.963	0.000	100.000
02	1.981	0.707	3.552	17.087	0.603	0.715	75.354	0.000	100.000
02_cut	1.981	0.707	3.552	17.087	0.603	0.715	75.354	0.000	100.000
03	1.694	0.665	7.528	23.912	0.802	0.831	64.435	0.133	100.000
03_cut	1.696	0.666	7.538	23.944	0.803	0.832	64.521	0.000	100.000
04	2.279	1.099	0.740	10.823	0.547	0.474	84.038	0.000	100.000
05	2.118	1.620	5.624	19.423	1.606	0.705	68.904	0.000	100.000
05_cut	2.071	1.584	5.500	18.993	1.570	0.689	67.378	2.214	100.000
07	2.226	2.435	2.107	14.185	1.140	0.474	74.554	2.879	100.000
07_cut	2.258	2.470	2.137	14.388	1.156	0.481	75.623	1.486	100.000
08	1.860	2.601	2.989	12.869	1.204	0.291	78.186	0.000	100.000
08_cut	1.846	2.580	2.966	12.768	1.195	0.288	77.571	0.787	100.000
09	2.198	1.079	5.910	19.789	0.769	0.599	69.656	0.000	100.000
09_cut	2.198	1.079	5.910	19.789	0.769	0.599	69.656	0.000	100.000
10	2.254	0.829	0.666	11.535	0.474	0.406	83.835	0.000	100.000
11	1.930	0.591	1.682	11.936	0.892	0.496	82.473	0.000	100.000
11_cut	1.899	0.582	1.655	11.742	0.878	0.488	81.138	1.619	100.000
12_cut	1.658	0.908	0.000	13.080	0.000	0.470	83.884	0.000	100.000
13	2.130	1.062	2.470	14.905	0.963	0.562	77.908	0.000	100.000
14	1.613	0.659	2.784	13.557	0.630	0.537	80.220	0.000	100.000
14_cut	1.596	0.652	2.755	13.419	0.623	0.532	79.405	1.017	100.000
15_cut	1.961	0.636	2.107	13.962	0.669	0.534	79.223	0.908	100.000

Table 1: Major element oxides in wt% normalised to 100% as detected in the XRF.

As seen from the results of the table the main element Ca suggests the existence of calcite along with impurities, what could probably be quartz (SiO<sub>2</sub>) or clay material. The purity of the plaster seems to differentiate, with S01 being with the most fillings. The majority of the samples however, are consistent with high amounts of Ca. The fresh cuts made for the confirmation of the previous elements detected show little, if any, difference in their amount. Notably, for the samples 05, 11 and 14 Fe was detected indicating possibly the presence of iron (hydro)oxides.

The table 2 below, shows the trace elements detected by the XRF. Even though we see trace elements found in other examined plasters from the Aegean, Thera (Profi et al. 1977, 108) and Knossos (Profi et al. 1976, 34-35), such as, Cu, Zn, Mn and even Ni, elements like Sr, Mo and Ba are of higher quantity. This may probably indicate the local source of the fillings inserted, however that would need further investigation to be safely admitted.

Sample	MnO	CoO	NiO	CuO	ZnO	SrO	MoO <sub>2</sub>	BaO
01	215	46	0	0	9	12	122	66560
02	194	63	0	0	7	7	122	63144
02_cut	194	32	0	0	9	9	121	73615
03	324	2	8	15	14	117	27	9483
03_cut	324	4	23	32	20	132	22	9602
04	221	29	0	0	6	12	123	54470
05	169	60	0	0	5	7	121	72526
05_cut	169	7	13	33	22	100	31	11399
07	175	8	15	28	42	116	36	10378
07_cut	175	3	6	64	35	100	42	15523
08	896	63	0	0	4	12	122	64741
08_cut	896	3	5	80	30	89	43	17096
09	289	47	0	0	0	11	121	57699
09_cut	289	7	18	39	24	107	31	10777
10	307	4	16	28	13	85	26	9070
11	172	38	0	0	8	15	127	58124
11_cut	172	4	14	41	25	87	32	11137
12_cut	321	3	24	42	21	109	28	10466
13	198	37	0	0	5	12	123	58790
14	238	34	0	0	7	13	122	55687
14_cut	238	9	27	24	39	115	25	9760
15_cut	202	4	13	77	18	64	37	14067

Table 2: Table of the trace elements of mortars detected in XRF. Values are shown in *ppm*. (A complete table can be found in the appendix: Table 2)

The samples were then inserted in the scanning electron microscope not only to confirm the measurements of the XRF but also to get a clearer view of more areas of the sample regarding its composition and topography.

A table showing the mean values and standard deviation of the main elements Ca and Si for each sample was created (Table 3). The table shows differences in the main composition of the plasters, even though most of them seem to be of high purity with Ca above 94%. There is a small group of three samples (S06, S09, S10) that fall within the margin of 82-88% and one (S01) that stands out as the most impure.

Sample	SiO <sub>2</sub> (Mean)	SiO <sub>2</sub> (Standard Deviation)	CaO (Mean)	CaO (Standard Deviation)
01	15.09	10.25	78.66	15.54
02	1.63	1.28	98.37	1.276
03	2.09	2.45	94.99	2.25
04	2.45	0.36	96.17	1.21
05	4.08	3.81	94.89	4.80
06	7.38	2.91	87.5	2.63
07	1.35	0.41	97.2	1.30
08	2.42	0.50	95.93	1.92
09	8.95	0.31	82.47	3.97
10	7.65	8.51	86.71	5.81
11	4.1	7.11	95.89	7.11
12	2.54	2.12	94.57	3.13
13	3.77	1.69	94.93	1.87
14	3.14	1.13	96.08	0.82
15	2.03	0.73	97.19	0.51

Table 3: Table showing the mean values in %wt and standard deviations of each sample as measured in SEM.

For a clearer illustration of the results a biplot was created to visualize the ratio of CaO and Si<sub>2</sub>O in each sample. (fig. 6)

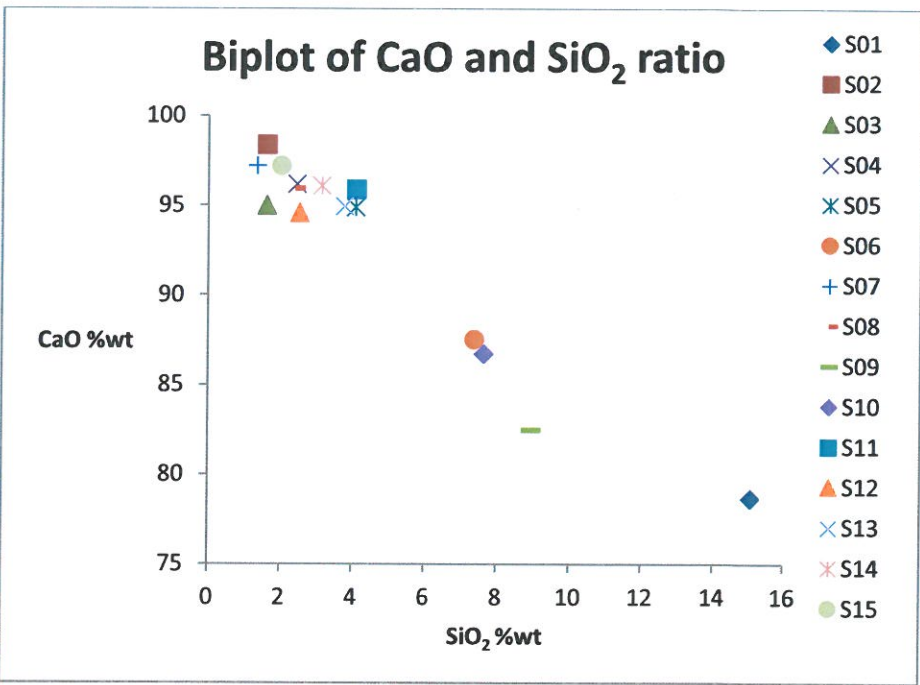


Figure 6: Biplot showing the ratio of CaO and SiO<sub>2</sub> %wt in the samples.

The sample 01 seems to be of lower quality since there are many aluminosilicates and little cohesion. (fig. 7) However, larger amounts of CaO (mean value: 78.66± 15.54) are detected in a bulk analysis (magn. x300) and less of SiO<sub>2</sub> (15.097±10.2). The interesting



feature is seen in spectrum 3 where Ca is almost 95%. The measurement was taken very near the surface, close to the pigment suggestive of a thin layer of fine plaster. (fig. 8)

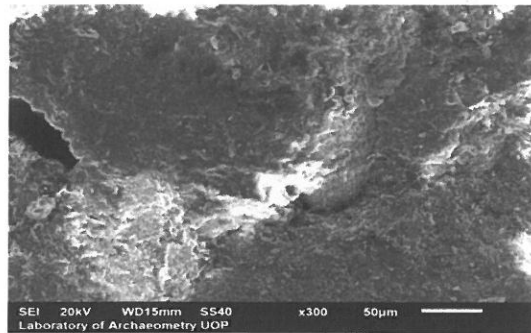
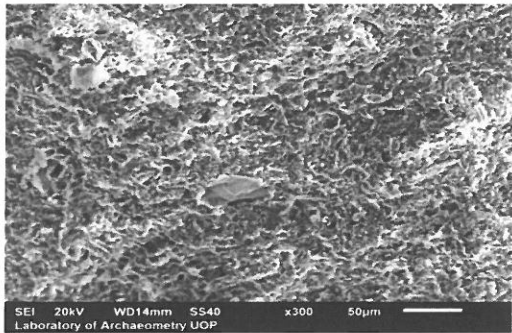


Figure 7: Sample 01, SEM. Mortar with pores and aluminosilicates.

Figure 8: Sample 01, SEM, mortar with tighter cohesion.

As for the samples 6, 9, 10 it seems that the cohesion of the material is analogous to the percentage of Ca. This is evident from the above measurements/biplot and the microscope images even if there is no big difference in quantitative results. (Figs. 9, 10)

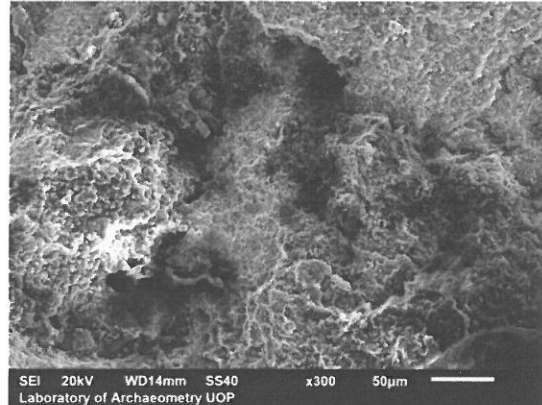
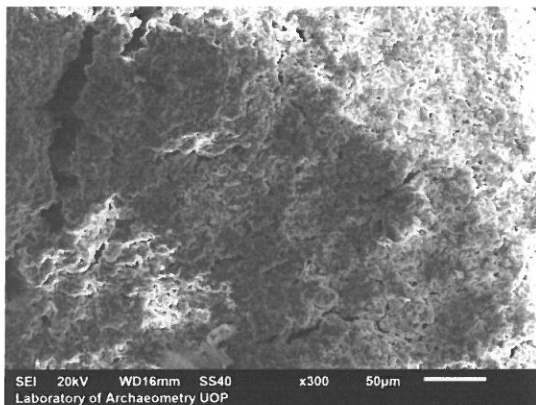


Figure 9: Left: Sample 06. Mortar, good cohesion, despite the few crackings. Right: Sample 09. Mortar, less cohesion of the material, cracks and holes observed.

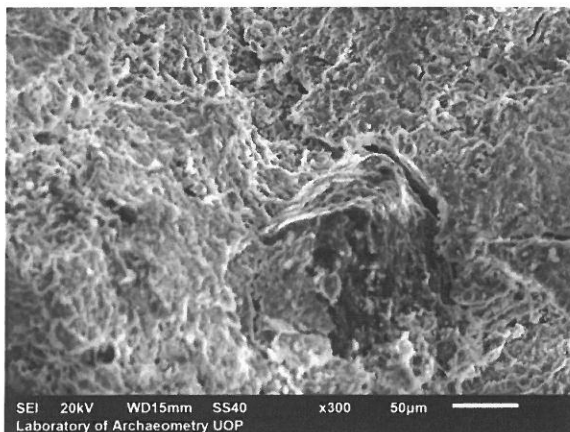


Figure 10: Sample 10. The structure of the mortar is continuous with few gaps and holes.

Of course some closer examination and spot analysis revealed that even in the purest plasters there are some times formations of salts as the existence of Na, Cl, and S suggests in sample 11. Furthermore, ferrous hydroxides are probably present in sample 10 since high amounts of Fe and Mn were detected. (fig. 11)

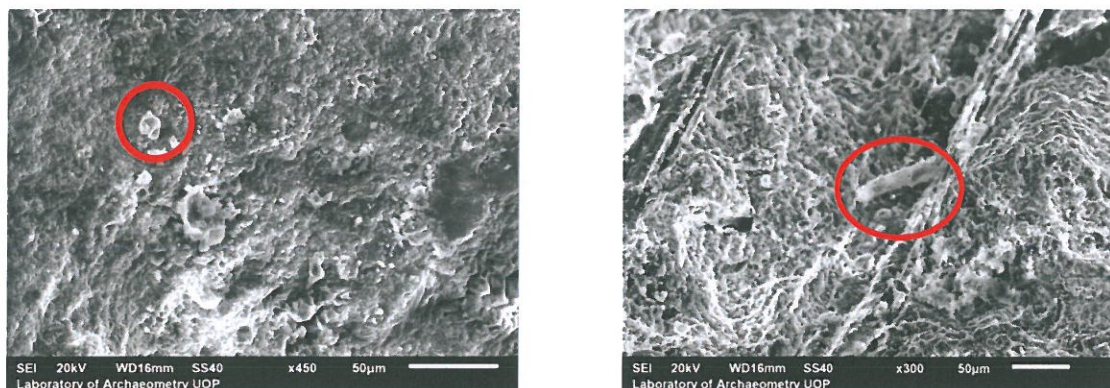


Figure 11: Left: Sample 11. Spot analysis on the grain of the above site of interest showed high amounts of Na, Cl and Fe. Right: Sample 10. The encircled formation is probably some ferrous hydroxide.

Further on, another biplot was created in an effort to demonstrate how fine grained is the mortar of the samples. The following table 4 shows the mean values in %wt of CaO, Al<sub>2</sub>O<sub>3</sub>, SiO<sub>2</sub> and the ratio of Al<sub>2</sub>O<sub>3</sub>/SiO<sub>2</sub> while the figure 12 demonstrates the ratio of CaO to that of Al<sub>2</sub>O<sub>3</sub>/SiO<sub>2</sub>.

Sample	CaO (Mean)	Al <sub>2</sub> O <sub>3</sub> (Mean)	SiO <sub>2</sub> (Mean)	Al <sub>2</sub> O <sub>3</sub> /SiO <sub>2</sub>
01	78.66	3.84	15.09	0.25
02	98.37	<i>BDL</i>	1.63	*
03	94.99	2.92	2.09	1.40
04	96.17	0.67	2.45	0.27
05	94.89	1.03	4.08	0.25
06	87.5	1.32	7.38	0.18
07	97.2	0.89	1.35	0.66
08	95.93	1.64	2.42	0.68
09	82.47	3.84	8.95	0.43
10	86.71	5.49	7.65	0.72
11	95.89	<i>BDL</i>	4.1	*
12	94.57	1.55	2.54	0.61
13	94.93	1.29	3.77	0.34
14	96.08	0.77	3.14	0.25
15	97.19	0.76	2.03	0.37

Table 4: Mean values of CaO, Al<sub>2</sub>O<sub>3</sub> SiO<sub>2</sub> in %wt as measured in the SEM and the ratio of Al<sub>2</sub>O<sub>3</sub>/SiO<sub>2</sub>. BDL stands for Below Detection Limit, while \* represents the lack of data.

From the table 4 can be seen that regarding the samples 02 and 11 the values of  $Al_2O_3$  were below detection limit. Consequently, the ratio of  $Al_2O_3/SiO_2$  could not be calculated as well. Therefore, the biplot is drawn for all the rest of the samples.

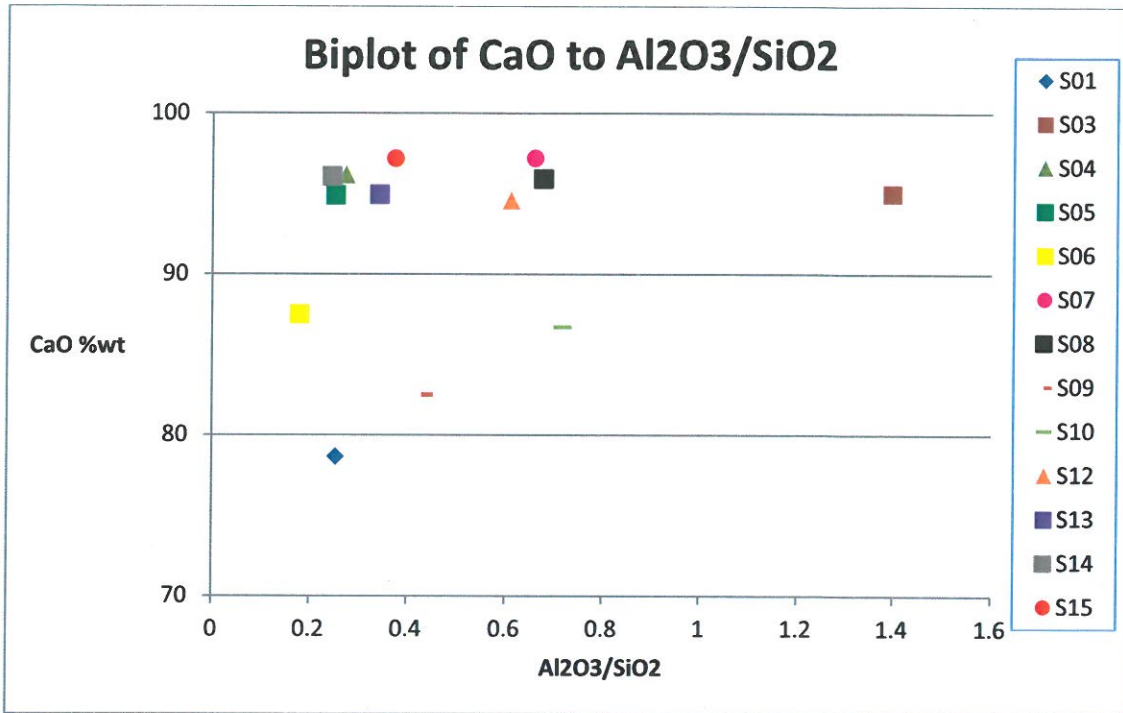


Figure 12: The biplot of the ratio of CaO to that of  $Al_2O_3/SiO_2$ . The values used are from the table above in %wt.

The biplot depicts the majority of the samples have fine-grained mortar (S04, S05, S13, S14, S15) or a little less (S07, S08, S12) with a high amount of CaO. Sample 03 despite its high CaO values is instead coarser, while to sample 01 are attributed the exact opposite characteristics. Not too surprisingly, samples 06, 09, and 10 once again stand on their own with lower CaO percentage but being within the frame of fine/medium fine grain.

Another biplot of the CaO/MgO was considered to see if more than one sources of Ca were used but in most of the samples MgO fell below the detection of SEM.

### 3. The Pigments

Regarding the pigments it should be generally stated that all of them with the exception of Egyptian Blue (EB) were prepared by natural raw materials. Consequently this restricted the colour palette of the Bronze Age painter, who of course employed various different ways to alter the hues of the basic colours available (dilution, concentration, finer grinding of the pigment grains). The use of coloured earth would of course include impurities that could enhance the final outcome. On the contrary, the need for purification of the raw material at hand was otherwise deemed essential. Naturally, these resources (apart again from EB) would be available in the local vicinity. (Morgan 2005, 209)

The palette of the Bronze Age painter included red, pink, orange, brown, yellow, black, white, grey, green, blue and purple. The macroscopic examination of the fifteen samples included a much smaller group of blue, pink, red, yellow, greenish blue and black. Sometimes a colour was superimposed on another to achieve a different hue.

The samples were first observed in the FOM microscope with x10 and x50 magnification. The pigment surfaces were overall weathered, with crusted dirt and the colour was in times flaked off. Of the most interesting cases is S01 showing a light blue surface with brighter blue grains. The same is obvious for S07 despite its darker hue. S07 shows clearly the case of *intonaco* where the pigment is placed on a thin layer of plaster. (fig. 13)

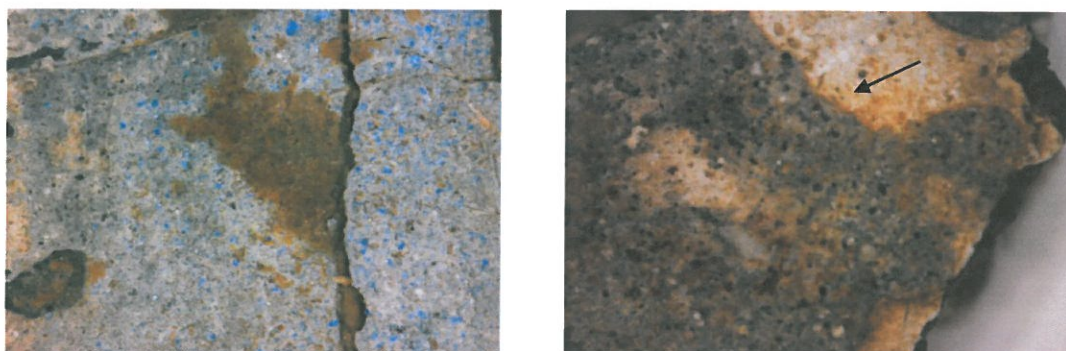


Figure 13: Left: Sample 01, LED magnification x50. Brighter blue grains in a cracked surface covered with compacted soil. Right: Sample 07, LED magnification x10. Dark blue surface with clear darker blue grains. The intonaco is showed by the arrow.

Our samples were then examined in the micro-XRF. The results however can only provide a qualitative estimation since the layer of the pigments was thin enough and the underlying mortar would affect the quantitative values credibility. For the same reason and

because the surfaces remained unclean the percentages provided by the SEM analysis should only be seen indicatively. Each sample will be presented with the measurements of both the micro-XRF and the SEM so as to provide an overall picture of the chemical analysis and confirm the results. For each sample during the SEM session, three spectra of bulk analysis were generated in different sites of interest. Then the mean values and standard deviations for each element were calculated and used.

### 3.1 Blue

Several of the samples had a main blue colour in several different hues. From the beginning it was hypothesised it was Egyptian blue (EB) pigment. This is what calcium copper tetrasilicate  $\text{CaCuSi}_4\text{O}_{10}$  is most commonly known and is considered the earliest synthetic pigment. It has been used for thousands of years, specifically from the 4<sup>th</sup> dynasty in Egypt until the Roman times (Eastaugh et al, 2004). Egyptian Blue shows a deep marine hue that is dependable on the particle size, the amount of copper and the fritting procedure. Consequently, the size of the particle can be between 20-100 $\mu\text{m}$  directly proportional to the intensity of the final colour (Profi et al. 1977, 112).

The preparation of the pigment was achieved by heating powdered limestone with a copper alloy (filings or an ore) and the addition of silica and soda or a plant-derived potash in temperatures of 850-1000°C. The product was then further refined by grinding. In the city of Tell El-Amarna (capital founded by Akhenaten of the 18<sup>th</sup> dynasty) workshops have been uncovered along with raw material and firing pots (Eastaugh et al, 2004). XRF analysis is indicative of EB by noting the presence of Cu (major element), a little less Ca and traces of Sn. (Profi et al. 1977, 112).

Egyptian Blue is not the only type of blue pigment in use. Another is that which derives from amphiboles. There are two types of amphiboles that give a blue colour although admittedly not as deep as the one of the EB. The first one is riebeckite,  $\text{Na}_2(\text{Fe}^{2+}\text{Mg})_3(\text{Fe}^{3+})_2\text{Si}_8\text{O}_{22}(\text{OH})_2$ , which is a rich in iron mineral of dark blue colour (Eastaugh et al, 2004). According to V. Perdikatsis the Theran blue of this type is most commonly Mg-riebeckite giving a dark blue-blue hue dependable on the Mg content. (Perdikatsis et al. 2000). The other amphibole is glaukophane meaning appearing blue in Greek. Glaukophane is a monoclinic silicate amphibole,  $\text{Na}_2(\text{Mg}_3\text{Al}_2)\text{Si}_8\text{O}_{22}(\text{OH})_2$ , with a blue-purple colour. The

metamorphosis of basaltic and sedimentary rocks under high pressure and low temperatures creates this type of mineral which is usually found along with riebeckite (Eastaugh et al, 2004). Glaucofanite is identified by XRF (major element Fe with little Cu presence), microscopy and XRD patterns. Of course, in the cases where EB is scarcer there is found a combination of EB and amphibole blue in which case the quantitative results give a 50-50 ratio of the basic parts (Profi et al. 1977, 112).

Our first sample s01, has a light blue hue and the figure 14 below is its XRF spectrogram.

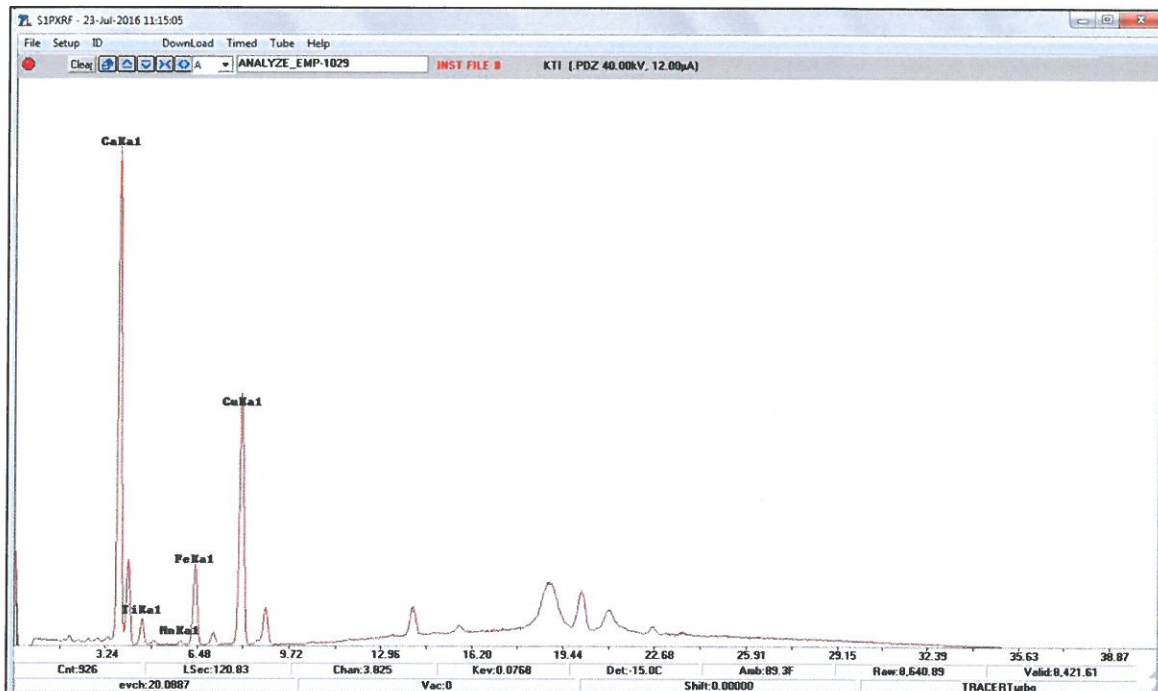


Figure 14: XRF spectrogram of S01.

The figure shows that Ca is our major element and Cu is the second followed by Fe and lower values of Ti and Mn. The elevated levels of Ca are mainly because of the underlying plaster however, this indicates the pigment is EB.

The SEM bulk analysis seems to corroborate this result. On the table 5 below are shown the elements detected by the SEM. It is clear that we have significant aluminosilicates because of the compacted dirt and the formation of salts probably because of the environmental conditions. The levels of Ca, Cu and Si would confirm that the pigment used is indeed EB. The light blue hue of EB could be because of the particle size after the grinding preparation or because of the initial raw materials (microstructure and components).

Sample 01	Al	Si	K	Ca	Fe	Cu
Mean	4.67	41.09	0.94	46.87	1.6	4.83
Standard Deviation	0.32	7.84	0.52	8.64	0.42	2.71

Table 5: Chemical analysis of s01 in SEM. Mean values and standard deviation. All results are shown in compound% and are normalised.

The next sample that is considered to have EB pigment is the half dark blue part of s04. The XRF analysis shows Fe as the major element if we consider Ca to be mainly from the substratum. Then follow Ti, Mn, Cu and Zn in lower levels. These would suggest the possibility of EB.

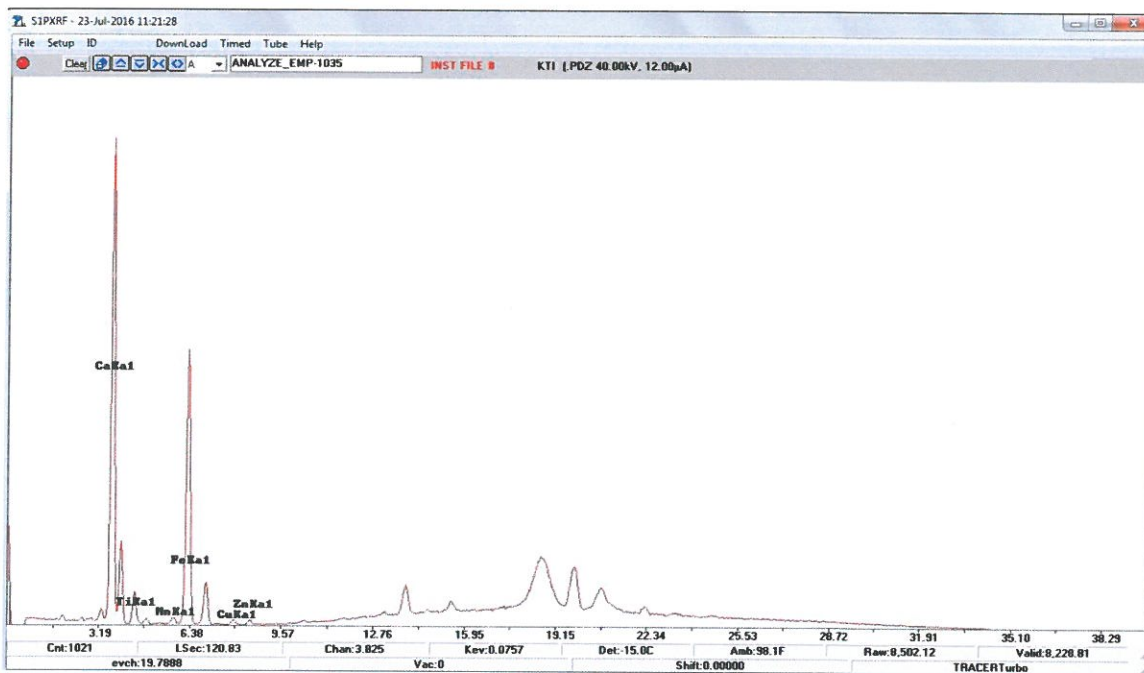


Figure 15: XRF spectrogram of S04 – dark blue.

The SEM gave quite different results (table 6). Excluding aluminosilicates as dirt, Ca because of the mortar beneath and the salts we basically have some amount of Fe and Mg. Copper was not detected at all, nor the other elements of the XRF spectrogram. However, the levels of C were high and it is probable we have a thin layer of EB coated over a black surface, since the other half of this sample is of that colour to darken the blue hue. In this case, the presence of pyrolusite ( $MnO_2$ ) is speculated. Of course C is detected because of the mortar beneath as well.

Sample 04 blue	Na	Mg	Al	Si	Cl	K	Ca	Fe
Mean	4.18	1.99	20.43	43.15	1.75	3.53	23.35	1.28
Standard Deviation	2.32	0.42	0.81	1.81	0.66	0.46	5.18	1.01

Table 6: Chemical analysis of s04 dark blue in SEM. Mean values and standard deviation. All results are shown in compound% and are normalised.

The next blue sample is s05. The surface of the pigment is in places flaked and covered with an amount of dirt. The XRF spectrogram indicates Fe as the major element followed by Ti and Mn, if it is assumed that the spike of Ca is because of the mortar (fig. 16).

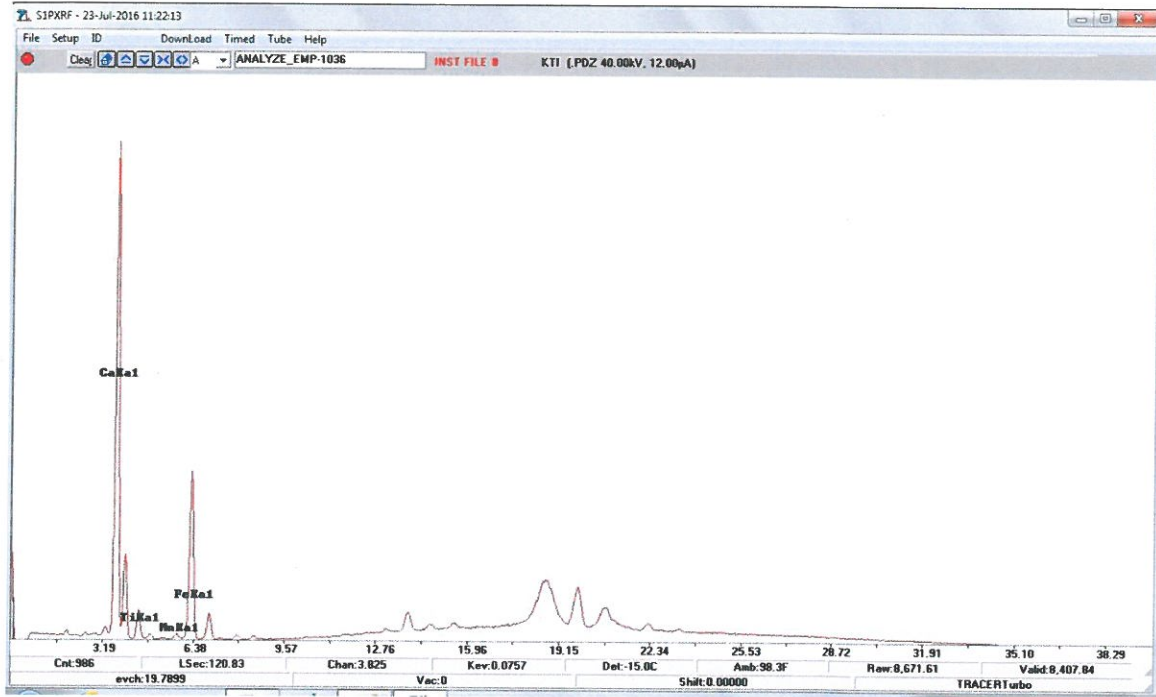


Figure 16: XRF spectrogram of S05.

The SEM bulk analysis detected the elements as seen in the table 7 below. Again excluding the aluminosilicates, chlorine and salts that come from the crusted dirt we are left mainly with Fe and a little bit of Cu. It could be proposed that the pigment is a type of amphibole blue, particularly that of glaucophane mainly because riebeckite is usually associated with some amount of Mg as well. Glaucophane can be identified by XRF having Fe as a major element with traces of Cu (Profi et al. 1977, 112). However, glaucophane as a natural mineral is not found in the Peloponnese. It has only been identified in Crete and Santorini and nowhere near the Mycenaean palaces of southern Greece. Its use in Knossos was violently put to an end c. 1.500 B.C. probably because of the volcanic eruption (Filippakis et al. 1976, 149). Until very recently, it was believed that Mycenaeans must have used EB nearly exclusively. However, relatively recent research done by Brysbaert and Perdikatsis (2008), has eventually shown the use of what is probably riebeckite along with EB in Mycenae, Thebes and Tyrins. This of course leads to the assumption if riebeckite was used why not glaucophane as well? The probability of an amphibole blue is also stressed by Brysbaert (2008) for the three aforementioned sites while Gla and Orchomenos continue to



use EB exclusively. Finally, further examination must be made to safely conclude about the specific pigment.

Sample 05	Na	Al	Si	Cl	K	Ca	Fe	Cu
Mean	3.21	16.68	35.35	1.9	2.44	36.35	3.96	*Only one result of 0.31. The rest were BDL.
Standard Deviation	1.65	5.59	12.79	0.37	0.76	17.97	0.42	

Table 7: Chemical analysis of s05 in SEM. Mean values and standard deviation. All results are shown in compound% and are normalised.

The XRF spectrogram of s10 gave impressive results with Cu being the major element, followed by Fe, Ca, Ti and Mn. This is safely suggestive of an EB pigment, while the high spike of Fe is probably explained by the dirt that covers nearly the entire surface of the sample (fig. 17). Alternatively, Fe is found in EB sometimes in substantial amounts indicating an intentional mixture, or it may have leached out of rusty iron tools, or lastly being present in clay material (Filippakis et al. 1976).

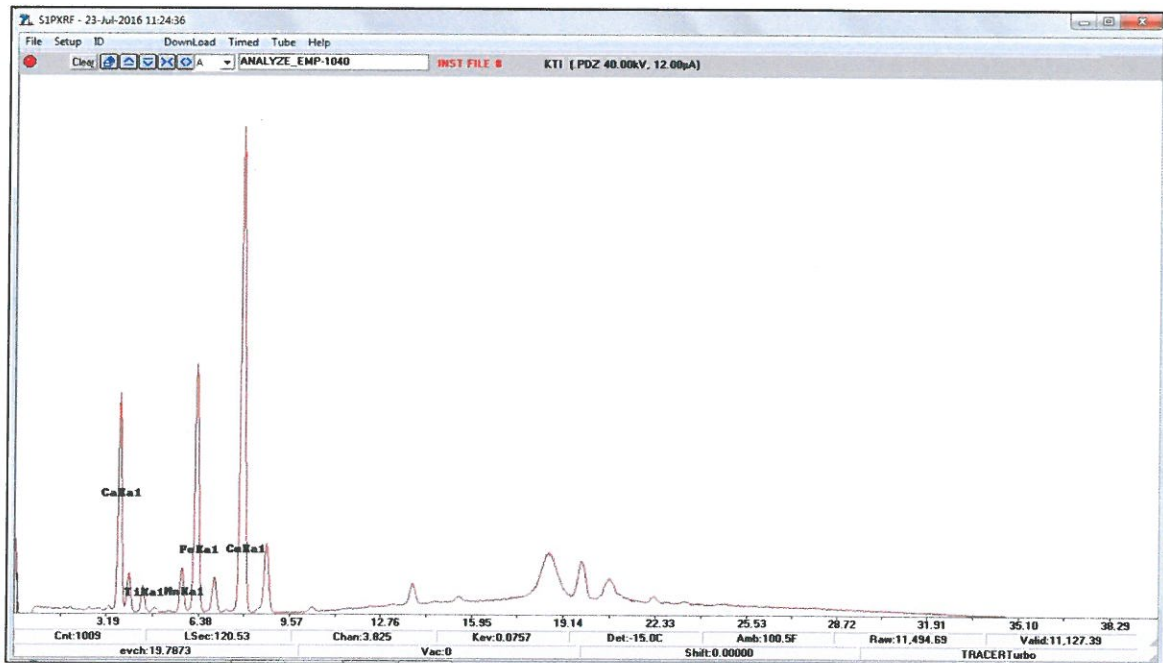


Figure 17: XRF spectrogram of s10

The same picture is given by the SEM bulk analysis with substantial levels of Cu and Fe, which helps to conclude that the pigment is EB. The rest of the elements should be partly attributed to the crusted soil and the underlying mortar (table 8).

Sample 10	Al	Si	K	Ca	Fe	Cu
Mean	4.14	43.96	0.82	44.12	3.06	3.90
Standard Deviation	3.49	10.44	0.84	15.61	2.31	2.02

Table 8: Chemical analysis of s10 in SEM. Mean values and standard deviation. All results are shown in compound% and are normalised.

Sample 11 presented a slightly difficult case due to its condition. Most of the colour had been scraped off revealing a white surface, and where the colour remained it was crusted with dirt. Only in one corner was the colour visible and its surface was somewhat small to locate during the SEM sessions. With that in mind, the XRF spectrogram revealed Fe is the major element followed by Ti and Mn. The spike of Ca is considerably high because of the exposed surface beneath and Fe could be partially attributed on the crusted soil (fig. 18).

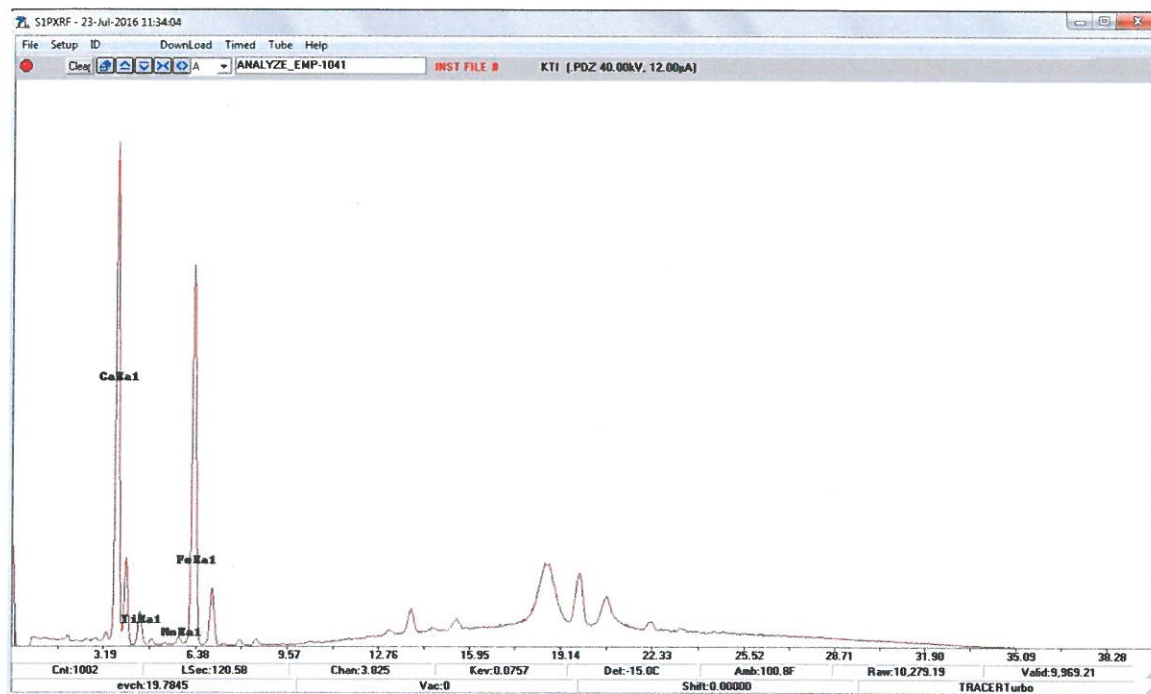


Figure 18: XRF spectrogram of s11

Under the SEM, apart from the aluminosilicates and the K a small amount of Cu was detected (table 9). The situation seems similar to the aforementioned of s05. However, in all the measurements C was significantly less than Ca. It is uncertain if Ca should even be partially attributed to the EB pigment when the result could be stemming entirely from the plaster itself.

Sample 11	Al	Si	K	Ca	Fe	Cu
Mean	13.82	34.65	2.35	45.85	3.12	0.59
Standard Deviation	5.37	16.023	1.04	23.27	2.11	0.56

Table 9: Chemical analysis of s11 in SEM. Mean values and standard deviation. All results are shown in compound% and are normalised.

Two more samples of blue colour were left for last, s02 (its half part) and s07. The XRF spectrogram for s02 shows Fe as a major element, followed by Ti and Mn (fig. 19).

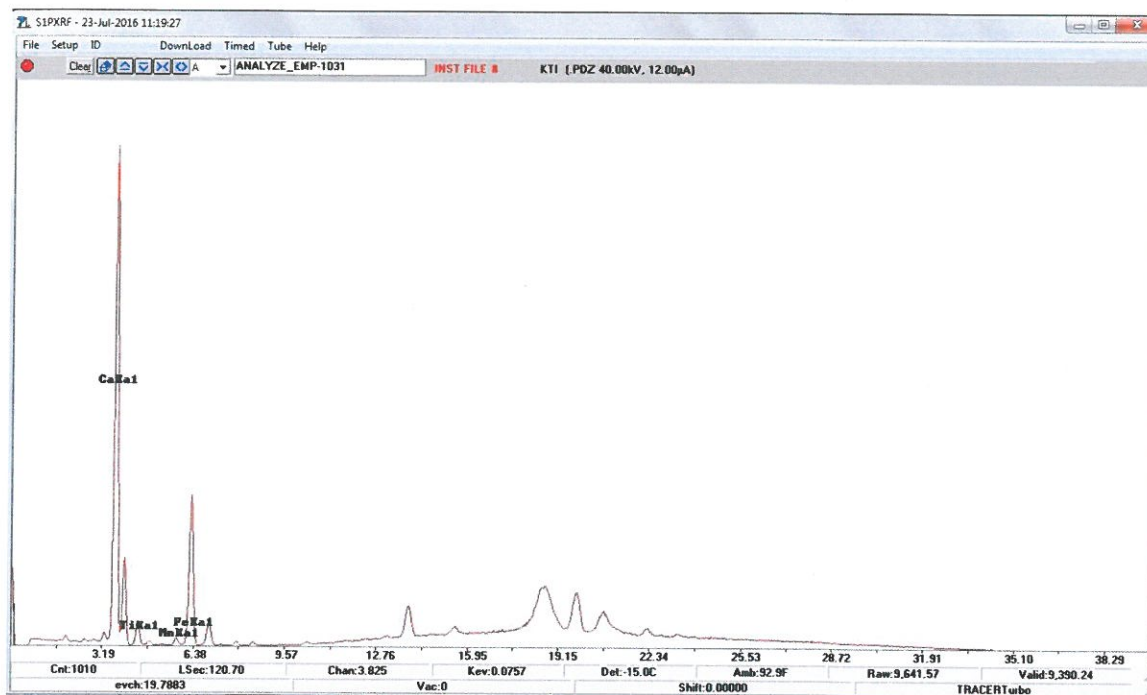


Figure 18: XRF spectrogram of s02-blue

Regarding the SEM analysis more or less the usual elements were detected with the total exception of copper. A little amount of Fe was found along with Mg and traces of Ti (table 10).

Sample	Na	Mg	Al	Si	Cl	K	Ca	Ti	Fe
02-blue									
Mean	2.1	1.77	17.12	39.85	1.07	2.69	32.31	0.55	3.31
Standard Deviation	0.67	0.85	3.317	10.67	0.85	0.27	17.23	0.34	2.33

Table 10: Chemical analysis of s02-blue in SEM. Mean values and standard deviation. All results are shown in compound% and are normalised.

As mentioned earlier another type of blue colour is that of amphibole. Given the dark blue hue of the pigment, the richness in Fe and the presence of Mg it should be surmised that s02-blue is not EB but Mg-Riebeckite blue. Besides, riebeckite has been probably identified in three mainland sites used solely and not mixed with EB (Brysaert, Perdikatsis, 2008). However, it is better if this is examined further to support this assumption with certainty.

The last blue sample is the small s07. The XRF spectrogram shows a spike of Fe followed by one little shorter of Ti and a substantially smaller spike of Mn. There is no evidence of copper while calcium must be solely from the underlying plaster.

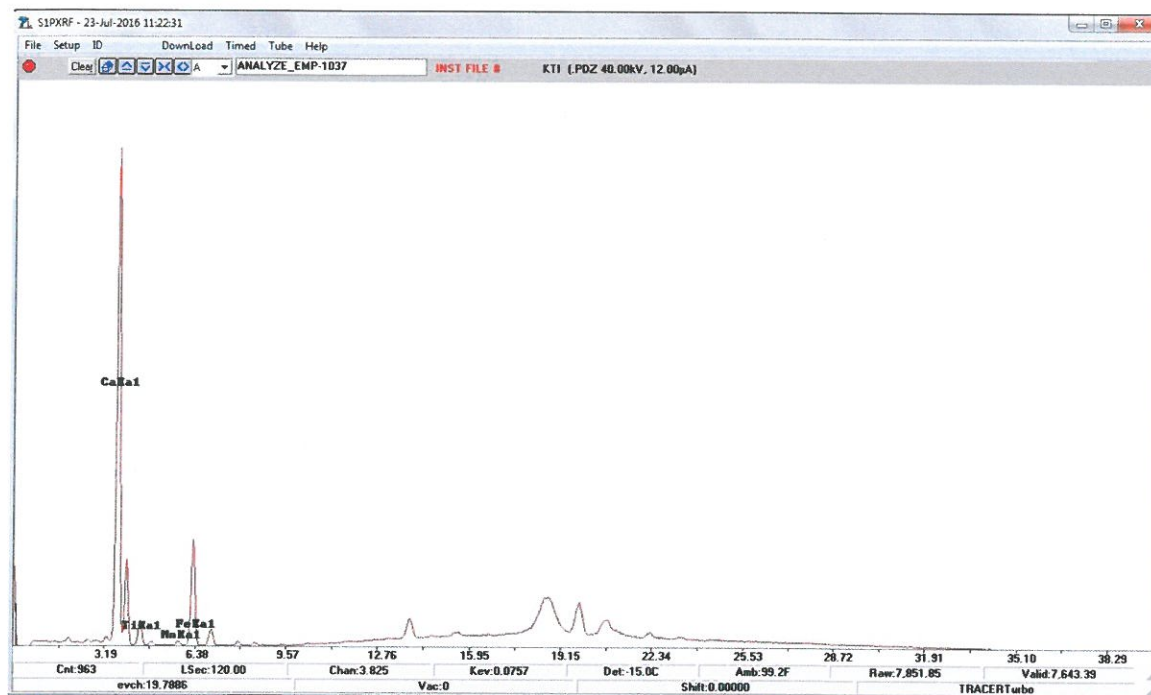


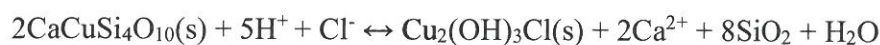
Figure 19: XRF spectrogram of s07.

The SEM analysis shows elements detected are those of s02 with the exception of Ti and although Fe is much less than in the previous sample, there is still enough of Mg. The conclusions for the pigment on this sample are the same as with s02. It is probably riebeckite though it has to be further examined to be safely confirmed.

Sample	Na	Mg	Al	Si	Cl	K	Ca	Fe
07								
Mean	3.50	1.76	22.64	43.06	2.08	2.49	21.39	3.07
Standard Deviation	0.77	1.28	1.42	4.45	0.59	0.27	5.44	0.87

Table 11: Chemical analysis of s07 in SEM. Mean values and standard deviation. All results are shown in compound% and are normalised.

Lastly, the grains of s06 had a light blue-green/turquoise hue. This was immediately suggestive of degradation of EB, which was examined further on. The degradation products of EB are atacamite,  $\text{Cu}_2(\text{OH})_3\text{Cl}(\text{s})$ , or its polymorphs, paratacamite or clinoatacamite. The degradation takes place when EB is found in high chlorine environment (Schiegl et al. 1989, Gimenez, 2015) through the following reaction:



The sample was examined in XRF and in SEM. The spectrogram below shows the elements detected on the XRF. There is a high peak for Ca probably because the pigment

layer is so thin, followed by Ti, Fe, Zn, Cu and Cl. The presence of Cl probably supports the supposition of EB degradation.

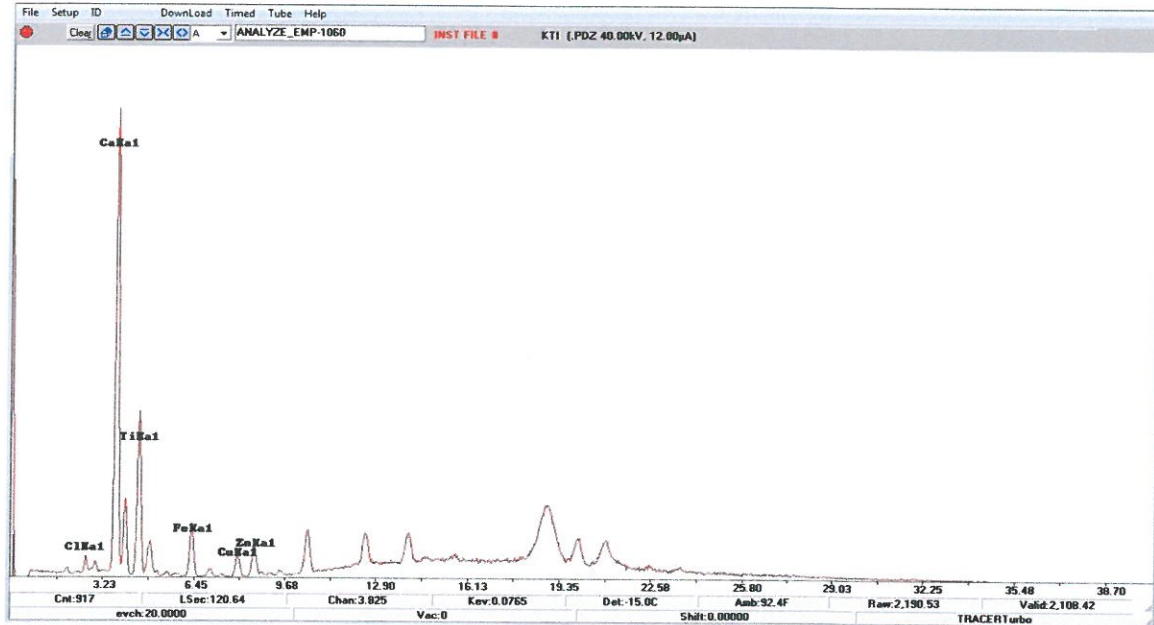


Figure 20: XRF spectrogram of s06.

The SEM analysis completes the data given by the XRF. It is impressive however, that the levels of Cl are less than every other element. There is substantial S and even Ti to pose the question if this is because of environmental conditions or if the ‘copper chloride cancer’ is not the case here. It should be noted however, that in order to positively identify atacamite as a degradation product of EB, the mortar should be separately examined. Only if sodium chloride salts are discovered in the mortar, it can be safely assumed that the EB has degraded. Atacamite has been identified as a raw material and as a sole green pigment in Hellenistic tombs. (Brecoulaki et al, 2006)

Sample	Mg	Al	Si	S	Cl	Ca	Ti	Fe
06								
Mean	4.44	10.86	25.70	5.88	2.20	39.03	8.78	3.093
Standard Deviation	1.23	1.65	2.62	2.84	0.77	1.80	3.03	1.51

Table 12: Chemical analysis of s06 in SEM. Mean values and standard deviation. All results are shown in compound% and are normalised.

### 3.2 Red

For the creation of the red colour XRF analysis done in samples from Knossos shows large amounts of Fe. Confirmation was provided by the XRD that spotted the presence of hematite. Inclusions of quartz in little amount, mica and clay minerals (biotite, muscovite) were also noted. (Profi et al. 1976, 37) Similar is the case in Mycenae, with the exception of one sample that showed some presence of Cu. (Profi et al. 1974, 109) In Thera however, Fe was the basic component along with Pb, Cr, Ti and Ba. Microscopic examination showed the presence of hematite ( $\text{Fe}_2\text{O}_3$ ) along with the iron hydroxide, the less lustrous goethite  $\text{FeO}(\text{OH})$ , in different analogies which relates to the different hue of the pigment. (Profi et al. 1977, 112) Perdikatsis in different Thera samples has identified hornblende as well, an indicator of the locality of the raw material since it is found in volcanic rocks (Perdikatsis 1998). The concentration of iron oxides is not the only parameter to influence the strength of the colour. The particle, the size and its shape along with the nature of the aluminosilicates affect the final outcome. For example high content of clay minerals can also affect the pigments plasticity and smoothness (Sotiropoulou et al, 2012).

There are three samples that their pigment is of red colour: the half of s02, s08 and s13. Regarding s02 it was examined first in the micro-XRF and then with the SEM. The qualitative analysis of the XRF results will continue to apply for all the samples. In figure 21 the XRF spectrogram shows a relatively high spike for Fe followed by those of Ti and Mn.

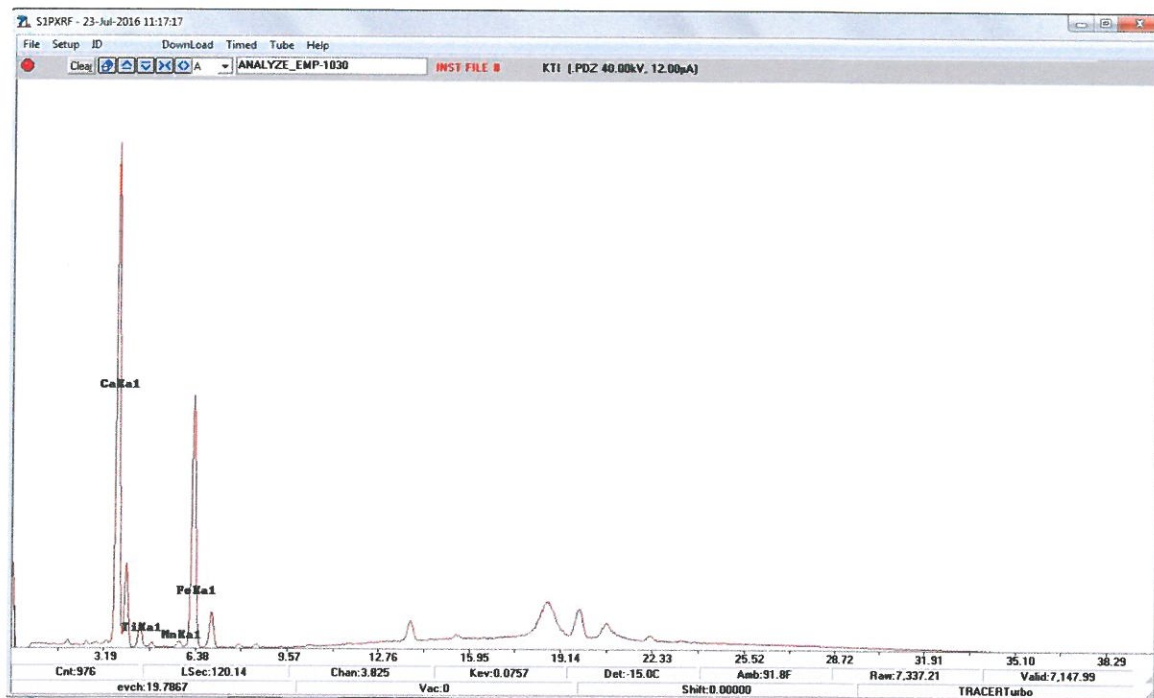


Figure 21: XRF spectrogram of s02-red.

The SEM results show several different elements with most striking the high percentage of Fe (table 13). From this it should be inferred that the pigment is an iron-rich earth ochre. Iron (hydro)oxides are very stable compounds that can be found anywhere on earth. They are suitable for pigment manufacture which is usually a strong and permanent colour. Such ochres are prepared by washing and grinding, they can be pure but they can also contain impurities such as clays, quartz or micas (Eastaugh et al, 2004). In this sample the chemical analysis seems to be in accordance with all of the above which is probably suggestive of an iron-rich ochre, speculatively of hematite with some impurities as seen by all the other elements present.

Sample 02-red	Na	Mg	Al	Si	Cl	K	Ca	Ti	Mn	Fe
Mean	2.19	1.92	22.35	50.35	1.93	2.99	8.91	0.70	0.13	8.53
Standard Deviation	1.01	1.63	2.15	1.57	0.88	0.47	1.57	0.79	0.12	0.86

Table 13: Chemical analysis of s02 red in SEM. Mean values and standard deviation. All results are shown in compound% and are normalised.

The next clearly red sample is s08. It has a reddish-brown hue and knowing that such colours come from red iron-rich ochres, this is what is expected in the measurements of both the XRF and the SEM examinations (fig.22, table14).

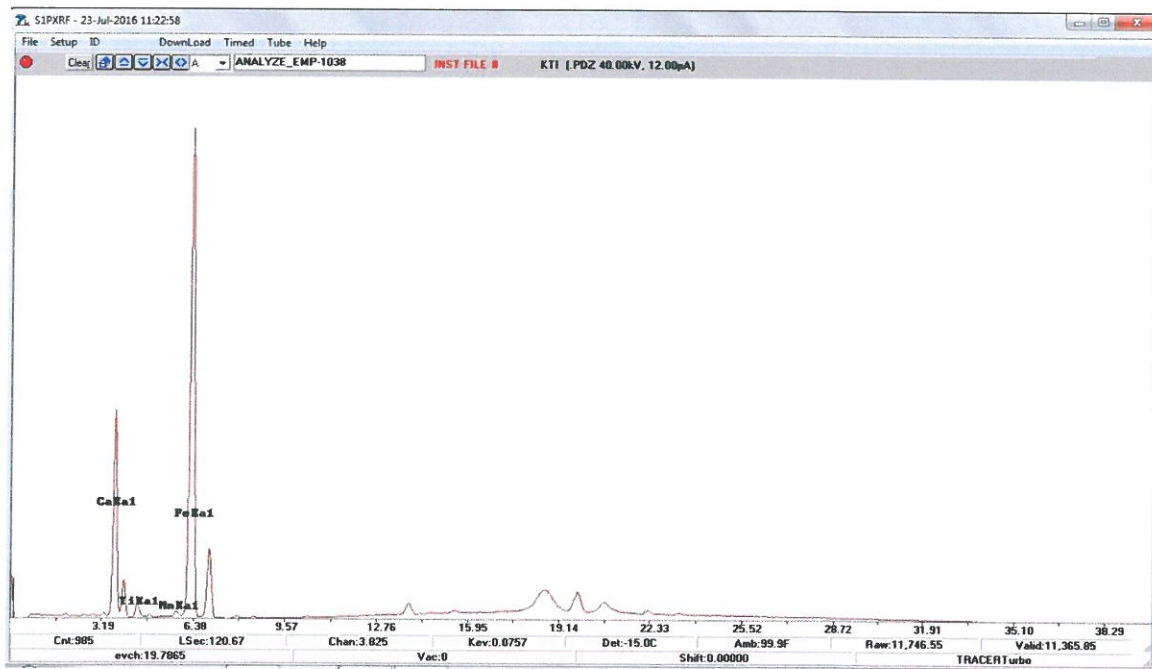


Figure 22: XRF spectrogram of s08.

The XRF spectrogram shows a very high peak for Fe, followed by a smaller one for Ca, Ti and Mn. This would suggest of a relatively thick layer and unaltered ferrous ochre in the composition of the pigment. Further on the results of SEM show the same elements detected as for the previous sample. The iron ranges between 1.31 and 8.71% thus giving such a mean value. It is once again speculated that the iron rich ochre, hematite is used as is bibliographically expected, with possible impurities.

Sample 08	Na	Mg	Al	Si	Cl	K	Ca	Fe
Mean	2.96	1.51	24.44	53.42	1.62	2.11	8.71	5.23
Standard Deviation	1.15	0.58	1.84	2.79	0.39	0.70	6.27	3.72

Table 14: Chemical analysis of s08 in SEM. Mean values and standard deviation. All results are shown in compound% and are normalised.

Things are not massively different for s13, except perhaps providing the highest values of Fe so far. The levels of Ca are also much higher than in samples s02-red and s08 probably meaning that the layer of the colour is thinner and the underlying calcite is more easily detected both in the XRF and the SEM (fig. 23, table 15). The pigment here consists of iron rich ochre, probably hematite, as well.

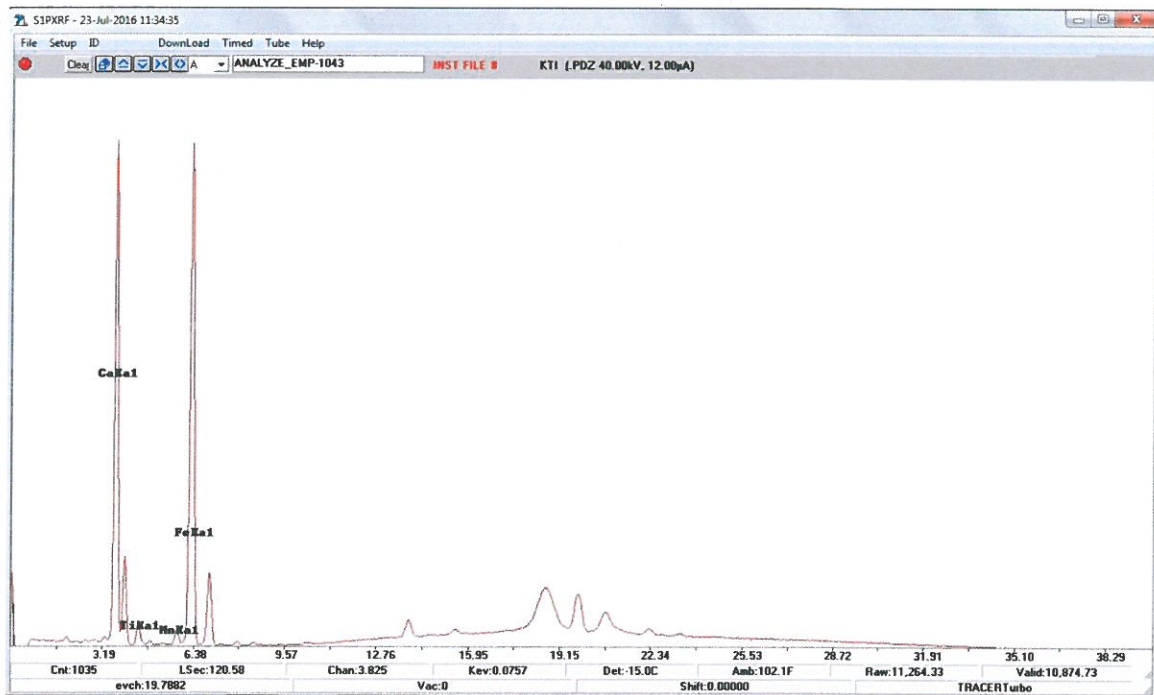


Figure 23: XRF spectrogram of s13.



Sample 13	Al	Si	K	Ca	Fe
Mean	15.37	34.59	1.29	32.95	15.8
Standard Deviation	1.88	4.12	0.33	3.42	3.63

Table 15: Chemical analysis of s13in SEM. Mean values and standard deviation. All results are shown in compound% and are normalised.

### 3.3 Pink

Pink colour is another one of the ochres composed by Fe oxides and Fe minerals. The XRF analysis of Theran samples showed presence of Fe which could only be confirmed microscopically, as clay, goethite, amorphous iron hydroxides and very few grains of hematite were spotted. (Profi et al. 1977, 112) The only difference in the Knossian samples was that under the microscope iron hydroxide, less hematite and some mica were found (Profi et al. 1976, 38). Pink colour was usually achieved by setting the red ochre on a lighter, white surface or was a result of hematite and other iron (hydro)oxides combined in different analogies (Profi et al. 1977, 112).

There are two samples that have macroscopically been indicated of having pink pigment, s03 and s14. Sample 03 showed signs of a little flaking and was a little coated with soil. It was examined in the XRF giving the following spectrogram (fig. 24). A significantly high peak for Ca is followed by that of Fe and the much shorter of Ti and Mn. This would suggest that the pigment is an iron compound but probably its layer is too thin and the underlying calcite of the mortar is easier detected or that the red ochre is mixed with calcite to create a lighter hue.

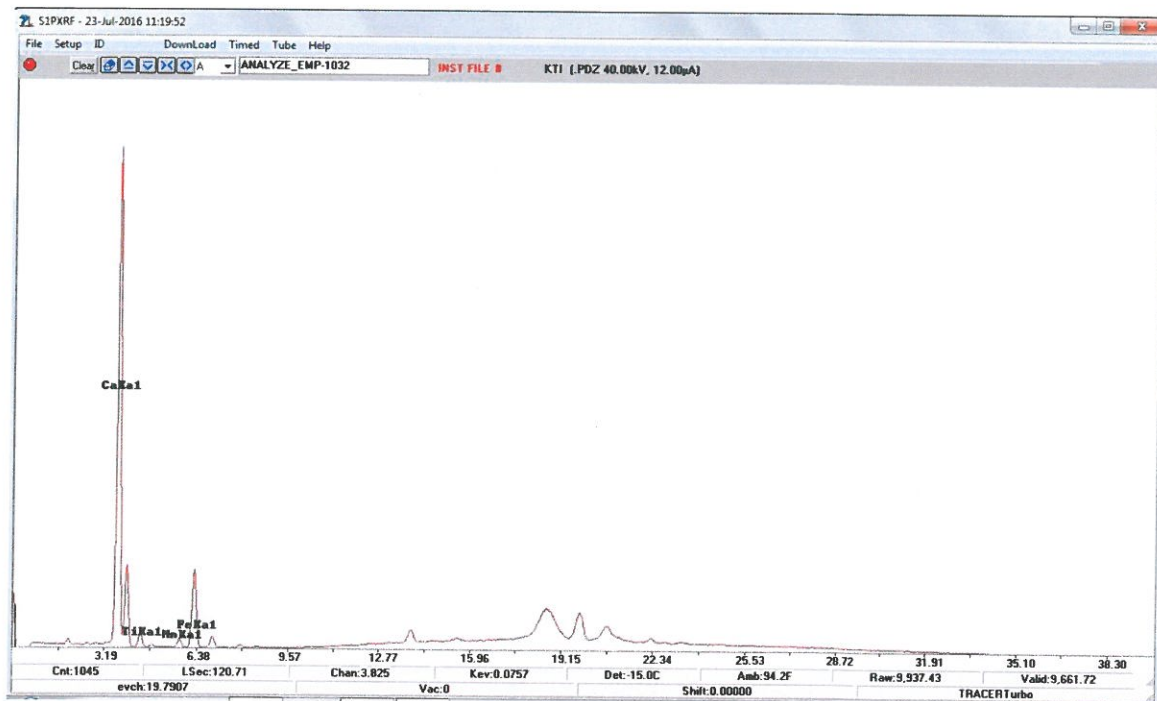


Figure 24: XRF spectrogram of s03.

The results of SEM show quite the same in regards to Fe (that could be hematite) and Ca. The rest of the elements should be considered either as impurities of the soil or perhaps as far Al and Si is concerned indication of clay.

Sample 03	Na	Al	Si	Cl	K	Ca	Fe
Mean	2.45	12.82	27.20	1.9	2.31	49.18	4.14
Standard Deviation	0.65	2.35	7.13	0.52	0.38	8.17	1.16

Table 16: Chemical analysis of s03 in SEM. Mean values and standard deviation. All results are shown in compound% and are normalised.

Regarding s14 more or less the same things can be said about its XRF spectrogram and the SEM results (fig. 25, table 17).

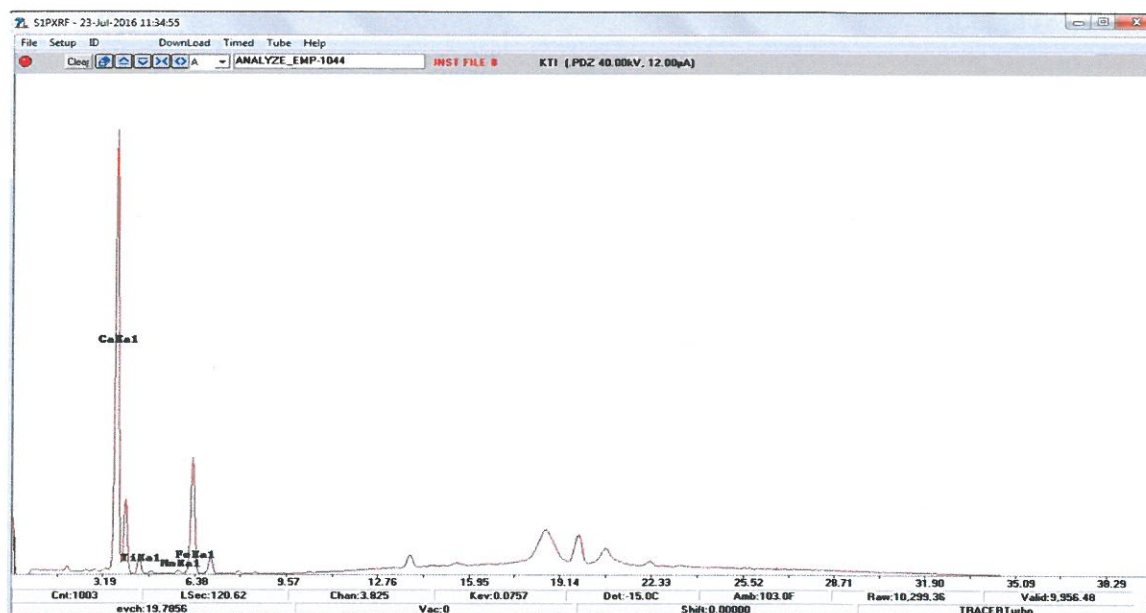


Figure 25: XRF spectrogram of s14.

The results of the SEM examination, show that in fact there is a little less Fe, substantially less Ca, while Al and Si have higher values. This would probably suggest the pigment is derived from an iron rich source; however it is probably more impure and may have more clay particles and minerals. The rest of the elements can be explained as elements found in the soil at the samples surface.

Sample14	Na	Mg	Al	Si	Cl	K	Ca	Fe
Mean	3.95	2.75	25.02	53.63	1.79	2.98	7.29	2.58
Standard Deviation	0.70	0.95	3.08	3.99	0.91	0.49	1.40	1.83

Table 17: Chemical analysis of s14 in SEM. Mean values and standard deviation. All results are shown in compound% and are normalised.

### 3.4 Yellow

Yellow is too one of the ochres consisted mainly of Fe. Therefore, it is not surprising that hematite is again the main colourant while goethite and limonite were also spotted in less amount. (Perdikatsis et al. 2000) Limonite, with the general chemical formula  $\text{FeO} \cdot \text{OH} \cdot n\text{H}_2\text{O}$  describes poorly crystalline iron oxides, the deposits of which contain hematite, silica, organic phosphates and clay minerals (Eastaugh et al, 2004). Such being the case in Thera, the Knossian and Mycenaean samples vary very little. In Knossos amorphous iron hydroxide along with quartz was located and in Mycenae this was determined to be limonite with quartz and very few hematite crystals. (Profi et al. 1974, 109; Profi et al. 1976, 38)

Of the fifteen samples only one, s09, showed a yellow pigment hue. Its examination with XRF showed a pretty high spike for Fe, followed by that of Ca and the shorter of Ti, Mn, Zn (fig. 26). The spectrogram allows the assumption that an iron rich earth ochre had been used.

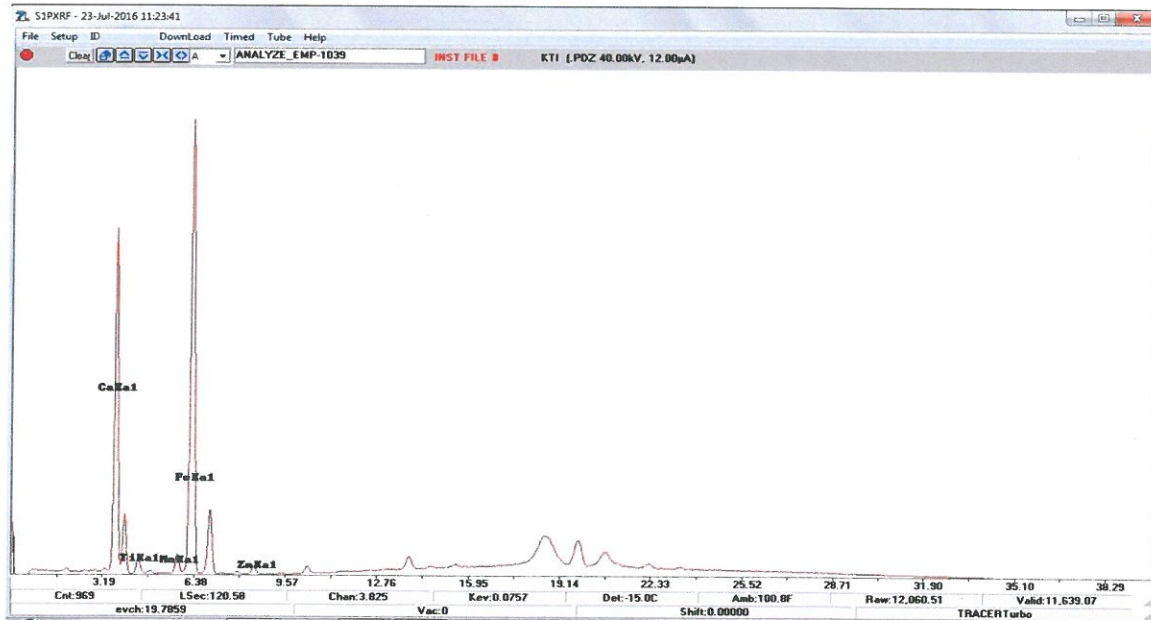


Figure 26: XRF spectrogram of s09.

The SEM results seem to validate the spectrogram. There is a substantial amount of Fe and Ca, with less Al and Si. It is probably clear that the yellow colour is provided by an iron (hydro)oxide, while the amounts of Al and Si indicate the existence of minerals and other clay materials. In this case, hematite, goethite and limonite are valid assumptions but further mineralogical examination is required.

Sample 09	Al	Si	Ca	Fe
Mean	6.32	15.14	58.39	20.16
Standard Deviation	1.86	3.32	7.49	4.98

Table 18: Chemical analysis of s09 in SEM. Mean values and standard deviation. All results are shown in compound% and are normalised.

### 3.5 Black

Black colour is produced by carbon based materials. These would include charcoal or bone ash. Lack of P indicates the use of wood coal. As such there are sometimes difficulties in their identification by certain analytical techniques (i.e. not detected in XRF). However, the mineralogical examination from Knossos distinguished two types. One includes black particles and some quartz and the other fewer black particles of smaller size with some brown iron oxides around them and nearly no quartz. (Profi et al. 1976, 36) The black particles are found together calcite, quartz, kaolinite but in Thera some feldspars and hornblende grains can be spotted, attributed to the volcanic land. (Perdikatsis 1993) Of course except from carbon derived black pigments there were also found some rich in Mn. Pyrolusite (Mn oxide) was found in a black pigment in Ayia Irini in Kea some other oxides in Santorini. Concerning the latter the specific samples have a more intense hue and the particles are not surrounded by brown iron oxides. The compounds are either MnO or Mn<sub>3</sub>O<sub>4</sub>. (Profi et al. 1977, 111). To all this Brysbaert (2008) adds a rare find of black made by the combination of magnetite (Fe<sub>3</sub>O<sub>4</sub>) and manganite (MnO(OH)).

There are three samples that have been identified as black, the half of s04, s12 and s15. Sample 04-black gave the following spectrogram in the XRF (fig. 27). The spectrogram shows a high Fe spike followed by that of Ca, Ti, Mn, Cu and Zn, which suggests the presence of some iron oxides and probably some clay minerals. The presence of MnO<sub>2</sub> (pyrolusite) is also speculated since it is not considered accidental, but it should be further investigated.

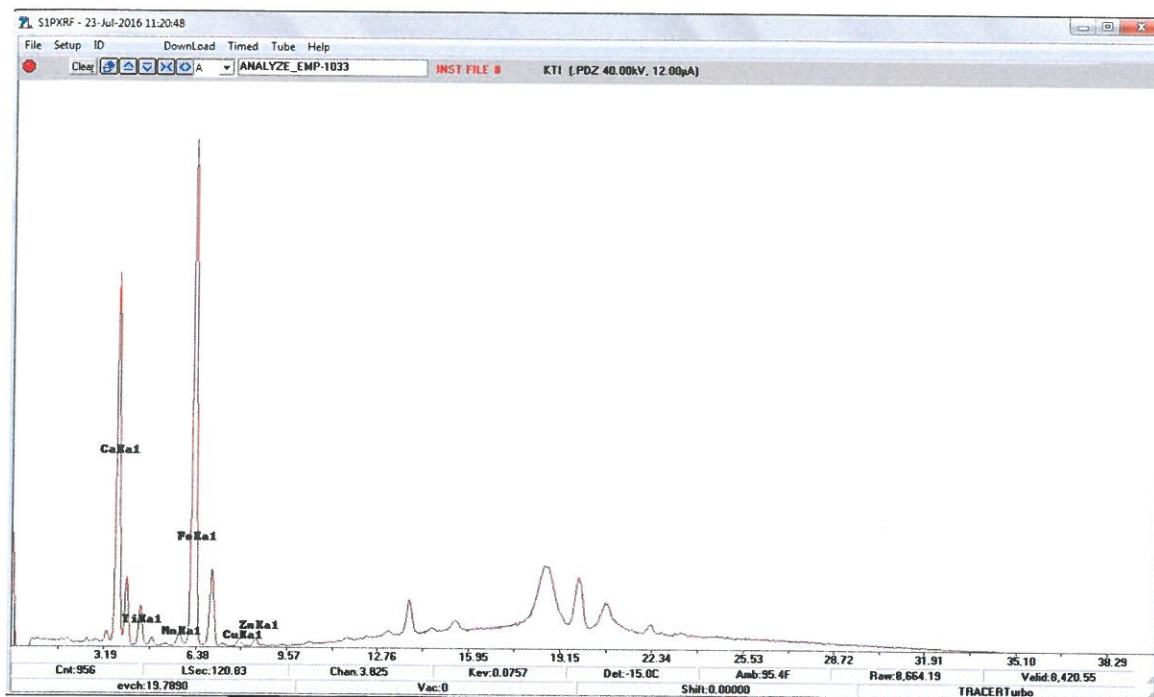


Figure 27: XRF spectrogram of s04-black.

The SEM examination gave however, relatively high amounts of C, little Ca and even less Fe (table 19). Having in mind that C may also be stemming from the substratum as does Ca, it can be assumed that the pigment is made mainly of carbon (plant ash). There is a possibility of existence of some iron oxides and clay minerals, while the rest of the elements are probably impurities found in the dirt of the sample's surface. If an identification of the minerals is required then further examination should follow.

Sample 04 black	Na	Mg	Al	Si	Cl	K	Ca	Fe
Mean	1.61	3.38	20.81	55.26	1.57	3.073	9.66	4.64
Standard Deviation	1.75	0.22	1.78	4.33	1.23	1.15	2.67	3.77

Table 19: Chemical analysis of s04 black in SEM. Mean values and standard deviation. All results are shown in compound% and are normalised.

The next sample, s12, was considered to have an overlying layer of black above a yellow one. This hypothesis was tested in the XRF. The spectrogram that follows (fig. 28) shows the highest peak belonging to Ca, followed by Fe, Mn and Ti. Smaller spikes still were identified for Ni, Cu and Zn. From this a hypothesis of carbon black cannot be excluded since C is undetected by the XRF, however, the existence of Mn might also indicate some pyrolusite or other Mn-oxide. The amount of Fe could also be connected with iron rich ochre for an underlying yellow stratum.

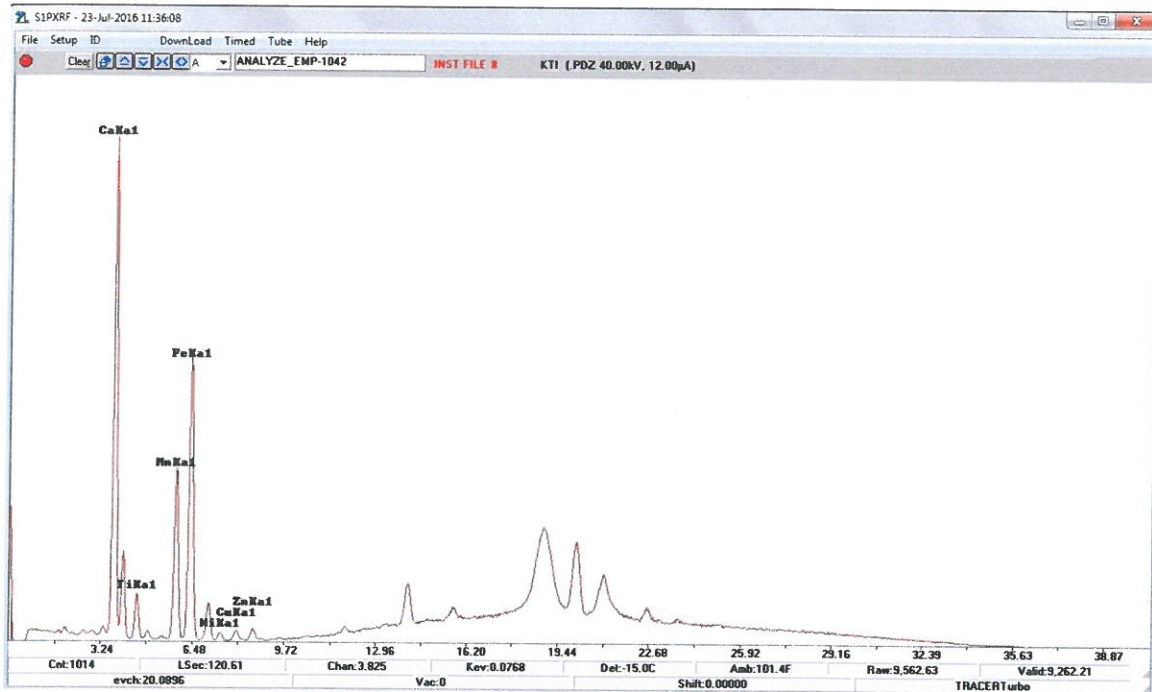


Figure 28: XRF spectrogram of s12.

The chemical analysis (table 20) of the sample is presented quite different however when examined in SEM. First of all, P is detected which seems to be in about the same level with C (in regards to the SEM spectrum). This of course completely alters the previous assumption. The carbon black here is derived from bone ash. Regarding the presence of Mn it indicates that the black pigment is probably composed of a Mn-oxide (pyrolusite) since were also found together with traces of Cu, Ni, Zn (Profi et al. 1977, 111).

In this sample the combination of carbon black and pyrolusite is considered unlikely. The pigment is probably made of an Mn-oxide and the P values are a speculated contamination. Finally, the levels of Fe could still be interpreted as colourants for a yellow substratum. This remains unclear and needs further examination.

Sample 12	Al	Si	P	K	Ca	Mn	Fe
Mean	16.97	38.07	11.33	3.48	16.39	5.95	7.81
Standard Deviation	2.51	5.01	3.34	0.52	5.46	2.03	1.35

Table 20: Chemical analysis of s12 in SEM. Mean values and standard deviation. All results are shown in compound% and are normalised.

The third sample with obvious black colour in one corner, s15 was then examined. Its XRF spectrum (fig. 29) shows high peaks for Ca, Fe, Ti and Mn. The height of Ca seems justified since most of the black colour has been flaked off and the XRF detects the main

element of underlying calcite. It is considered a probability that the pigment must be consisted mainly of Fe and Mn.

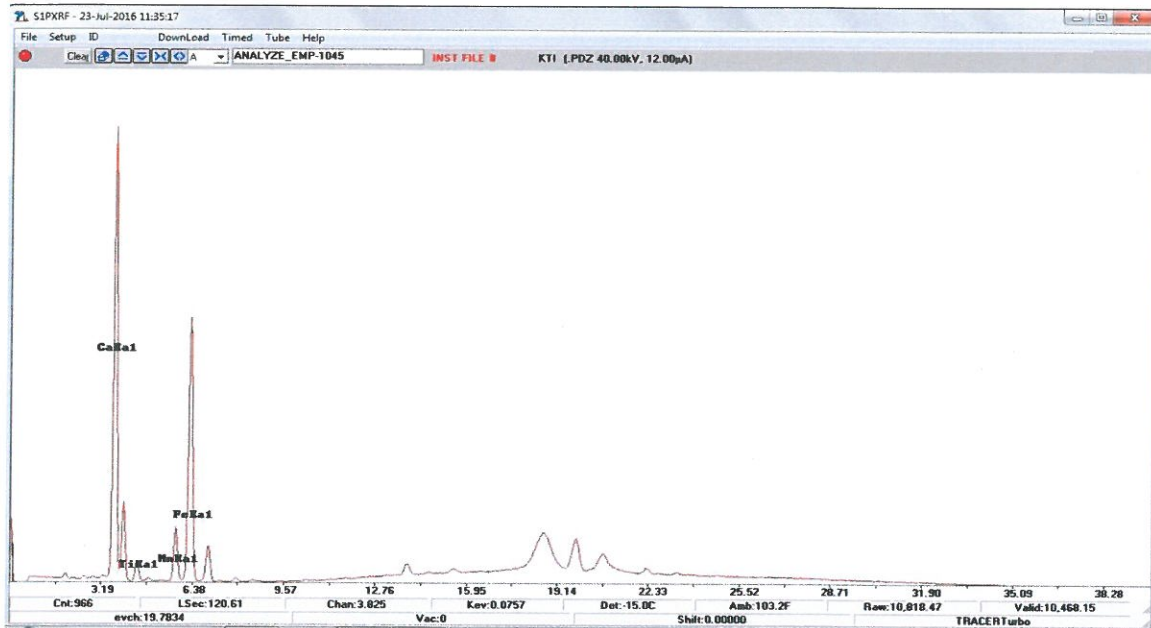


Figure 29: XRF spectrogram of s15.

To prove the previous statement a SEM analysis was done on the white part of the sample which gave the results of table 21:

Sample 15	Al	Si	Cl	K	Ca	Mn	Fe
Bulk analysis	0.62	2	0.26	0.24	94.07	1.9	0.91

Table 21: Chemical analysis of s15 in SEM. Mean values and standard deviation. All results are shown in compound% and are normalised.

The results differ substantially. All the values have decreased to a small amount, while Ca is c. 94% stemming directly from the plaster.

Sample 15	Al	Si	Cl	K	Ca	Mn	Fe
Mean	14.21	48.55	1.34	1.84	13.76	3.46	16.84
Standard Deviation	1.04	3.39	0.30	0.33	7.19	2.03	6.92

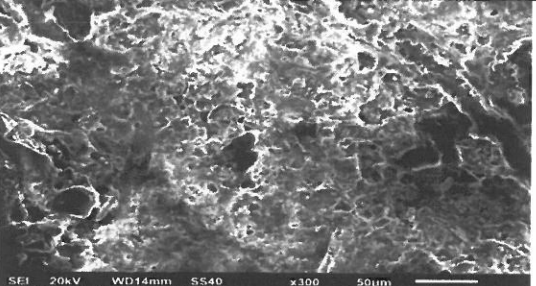
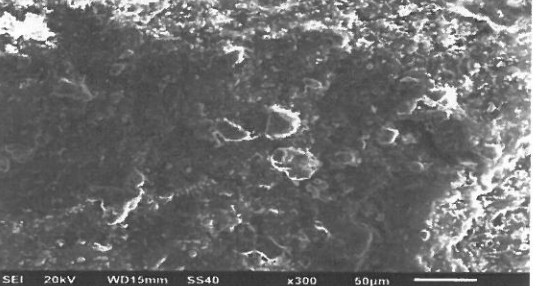
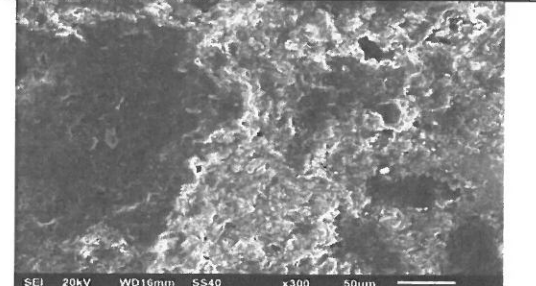
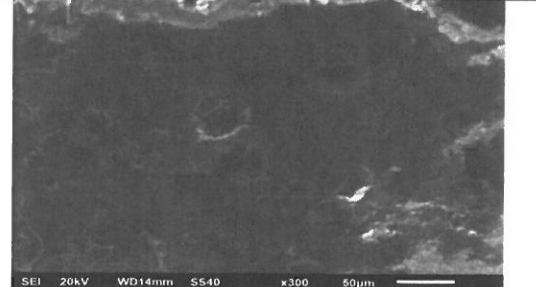
Table 22: Chemical analysis of s15 in SEM. Mean values and standard deviation. All results are shown in compound% and are normalised.

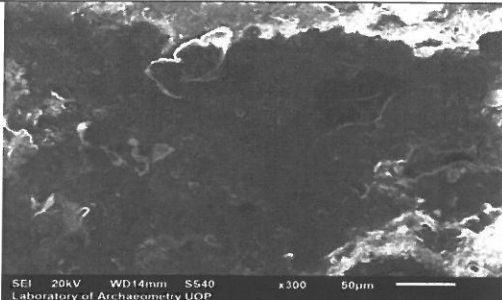
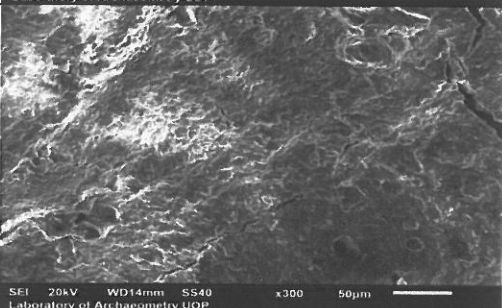
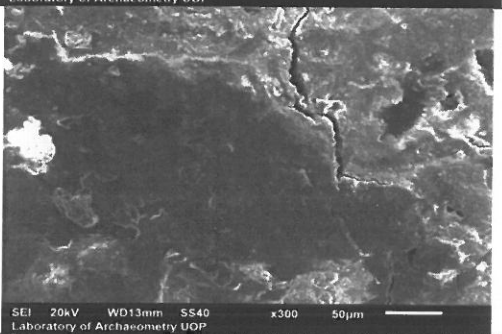
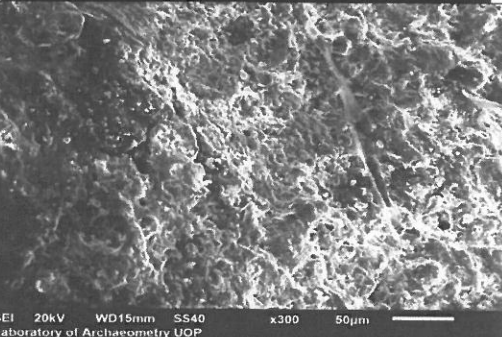
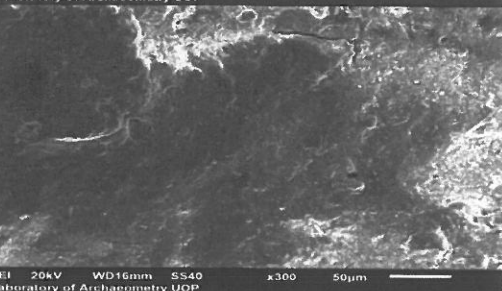
Therefore, everything else seen in table 22 comes from the pigment and the crusted soil it has. The elements K and Cl can be defined as simple impurities while Al and Si can originate from the soil or perhaps indicate a little amount of minerals. Carbon was noted to be quite high suggestive a derivative of plant ash. Finally, because of the significant difference of

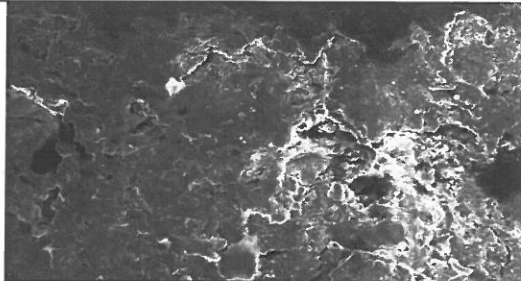
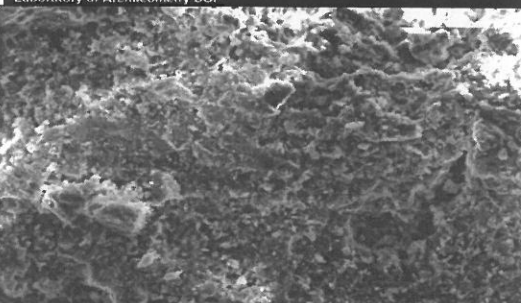
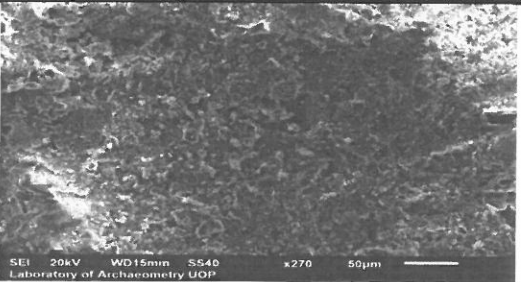
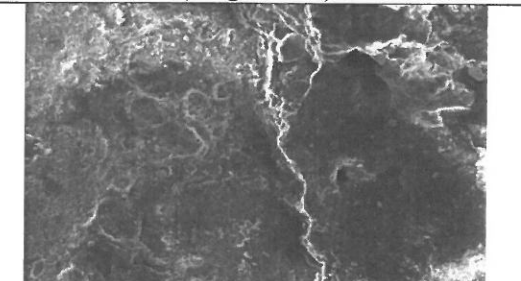
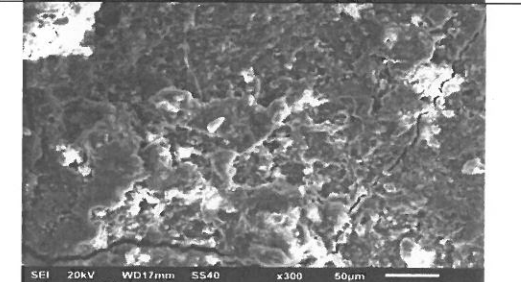


amount of percentages, it is considered possible that the black colour comes from an iron oxide (probably magnetite) as was the rare case in Phylacopi and Thebes (Brysbaert, 2008).

An illustrative summary of all of the above is presented below (table 23) along with indicative SEM images of the pigment surface. Apparently, each sample has its own distinct topography either quite coherent or with holes and cracks. In several cases, granular formations can be distinguished.

Sample/Colour	Pigment	SEM images of bulk analysis for pigments (magn x300)
01 Blue	EB	 <p>SEI 20kV WD14mm S540 x300 50µm Laboratory of Archaeometry UOP</p>
02 Red	Red ochre, hematite?	 <p>SEI 20kV WD15mm S540 x300 50µm Laboratory of Archaeometry UOP</p>
02 Blue	Amphibole, riebeckite?	 <p>SEI 20kV WD16mm S540 x300 50µm Laboratory of Archaeometry UOP</p>
03 Pink	Red ochre, hematite+calcite?	 <p>SEI 20kV WD14mm S540 x300 50µm Laboratory of Archaeometry UOP</p>

04 Blue	EB	
04 Black	Carbon black (plant ash)	
05Blue	Amphibole, glaucophane?	
06 Green-blue	Degraded EB, atacamite/paratacamite?	
07 Blue	Amphibole, riebeckite?	

08 Red	Red ochre, hematite?	 <p>SEI 20kV WD16mm SS40 x300 50µm Laboratory of Archaeometry UOP</p>
09 Yellow	Yellow ochre, hematite, goethite, limonite?	 <p>SEI 20kV WD14mm SS40 x300 50µm Laboratory of Archaeometry UOP</p>
10 Blue	EB	 <p>SEI 20kV WD15mm SS40 x270 50µm Laboratory of Archaeometry UOP</p> <p>(magn x270)</p>
11 Blue	EB	 <p>SEI 20kV WD16mm SS40 x300 50µm Laboratory of Archaeometry UOP</p>
12 Black	Carbon black (bone) + Mn-oxide?	 <p>SEI 20kV WD17mm SS40 x300 50µm Laboratory of Archaeometry UOP</p>

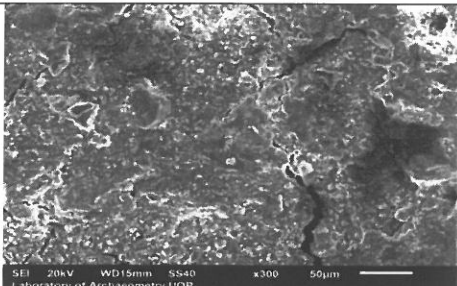
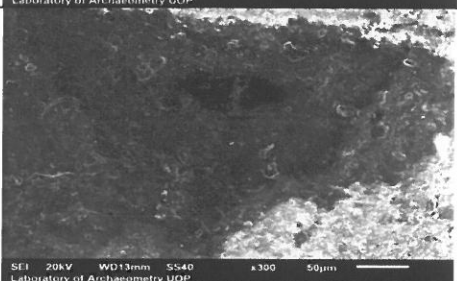
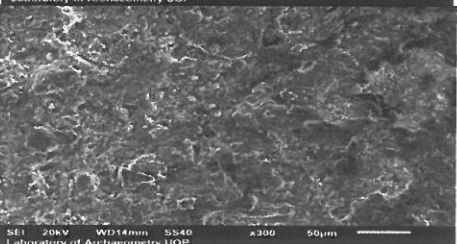
13 Red	Red ochre, hematite?	
14 Pink	Red ochre, hematite?	
15 Black	Carbon black and/or Black hematite?	

Table 23: Summative table of the sample pigments along with their SEM images.

In order to further examine the layers of the samples a few of them were cut and then moulded in resin in order to be examined in the backscattering electron mode (BSE) of SEM/EDS. The acquisition time for the results was set to 60s, while the accelerating voltage (20kV) and the spotsize (40) remained unchanged. The purpose here was to see if the pigment layer could be distinguished by that of the mortar, and possibly get a clearer elemental analysis.

The first sample that was examined was s01. With magnification x120 is visible a rough surface on the top of the sample (fig. 30 left). Several spectra were created for that area and the extending one below (fig. 30 right).

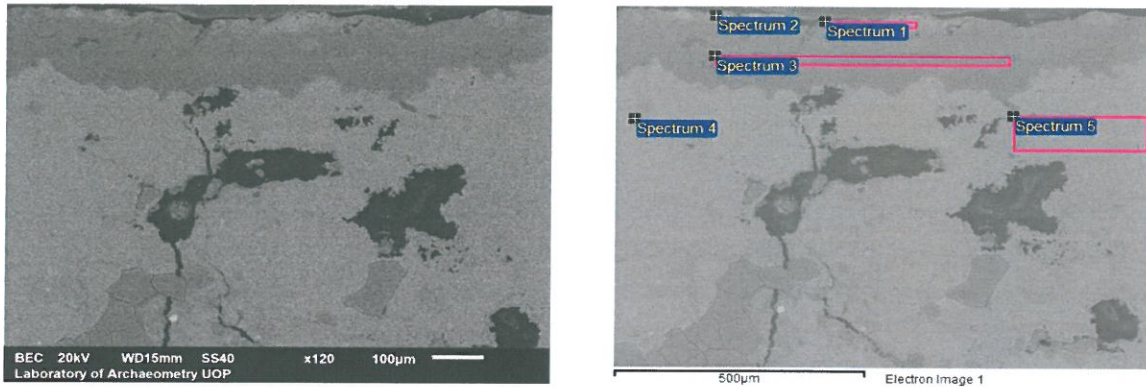
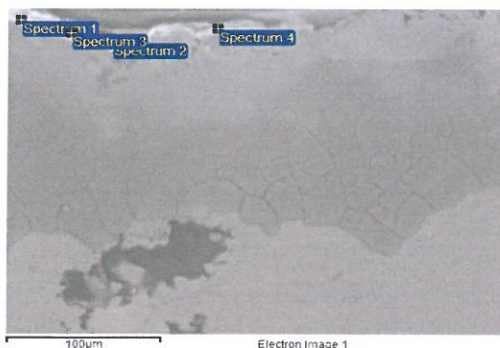


Figure 30: Left: polished surface of sample 01 in BSE, magn x120. Right: Spectra generated in several areas and spots.

Spectrum	Al	Si	Ca	Cu	Notes
Spectrum 1	2.41	16.07	81.52	N/D	
Spectrum 2	N/D	10.75	88.02	1.23	spot
Spectrum 3	0.02	76.65	22.63	0.71	
Spectrum 4	0.55	N/D	98.06	1.39	spot
Spectrum 5	0.67	3.62	95.71	N/D	

Table 24: Chemical analysis of s01 in BSE. All results are shown in compound% and are normalised.

What can be derived from the above is probably the fact that the top surface has some aluminosilicates from soil residue, while grains of copper can still be sporadically found from the pigment that had been coated. In a deeper level, entering that of the plaster the Ca value rises showing a clearer quality. Extra spot analysis on the surface seems to enhance the notion of soil between which pigment residue can be found (fig. 31, table 25).



Spectrum	Al	Si	Ca	Cu	Notes
Spectrum 1	N/D	75.37	24.63	N/D	spot
Spectrum 2	0.72	24.25	75.03	N/D	spot
Spectrum 3	1.88	68.99	28.68	0.45	spot
Spectrum 4	2.39	11.09	86.52	N/D	spot

Figure 31: Left: polished surface of sample 01 in magn x400. Right: Table 25: Chemical analysis of s01 in BSE. All results are shown in compound% and are normalised.

The second sample to be examined thereafter was s02-red. The top layer of the sample seems to be distinguished in texture, it is uneven and formed by grains. (fig 32).

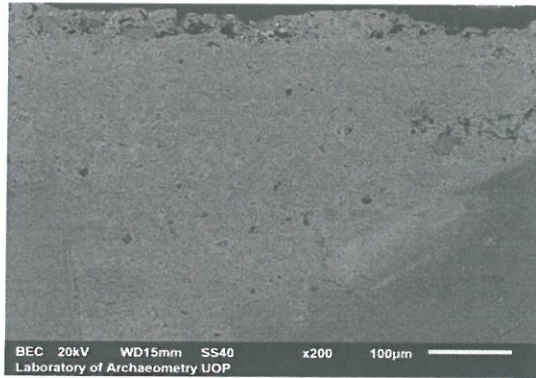


Figure 32: Sample 02 red in BSE, magn x200. Granural layer on top presents different cohesion to what is underneath.

The evidence of that being in fact the pigment layer is strengthened when a cracking deviding it from the substratum was noticed (fig. 33).

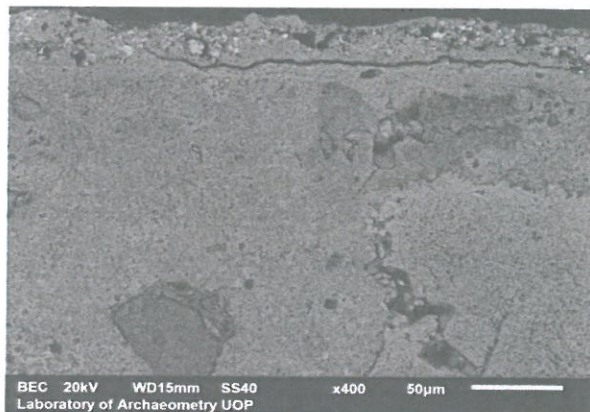
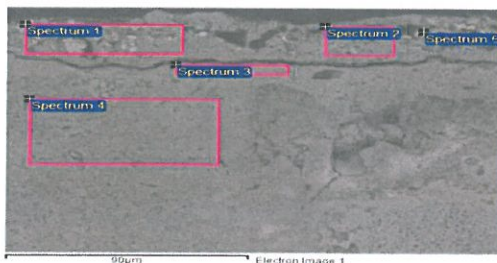


Figure 43: Sample 02 red in BSE, magn x400. Granural layer on top presents different cohesion to what is underneath, divided by a cracking.

Several spectra were created to test this hypothesis. The fig. 34 shows the areas that correspond to the analysis which is shown in table 26.



Spectrum	Al	Si	Ca	Fe	Notes
Spectrum 1	0.24	5.96	56.98	36.82	
Spectrum 2	0.69	2.75	75.97	20.6	
Spectrum 3	N/D	3.56	95.35	1.09	
Spectrum 4	N/D	1.29	98.58	0.14	
Spectrum 5	2.13	7.59	10.73	79.55	Spot

Figure 54: Sample 02 red, magn x400. Table 26: Chemical analysis of the areas of s02 red as outlined in fig. 34.

The results of the analysis show that the area above the cracking is consisted of the red ochre pigment since a large amount of Fe (red ochre) has been found as seen from the spectra

1 and 2. Furthermore, the spot analysis of spectrum 5 shows that this is an iron rich grain (likely hematite). The cracking seems as well to be dividing the two different layers. Underneath it the amount of Ca is increased over 95% showing that is the plaster area.

The last sample examined was s12. Viewing it under magnification x120 it can be clearly distinguished the upper layer of the pigment divided by that of the mortar underneath (fig. 35).

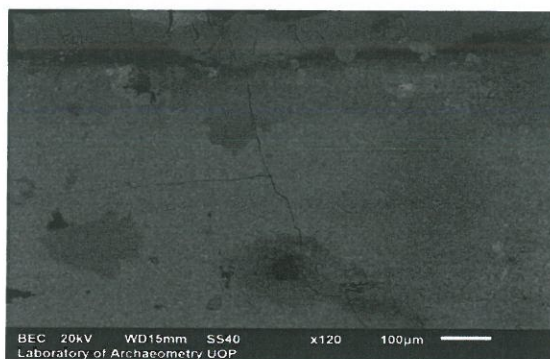
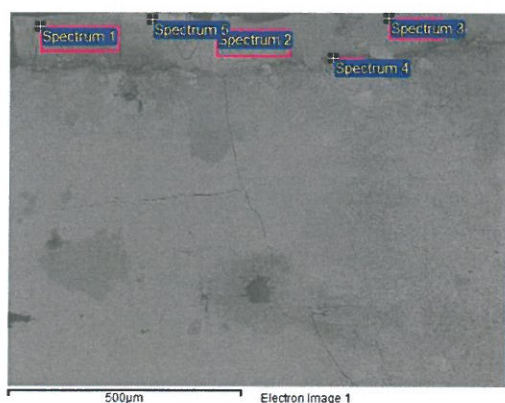


Figure 65: Sample 12 in BSE, magn x120. Distinct division of pigment and mortar layers.

Analysis was performed to study the chemistry of the surface. Figure 36 depicts the areas that the spectra correspond to and table 27 shows these results.



Spectrum	Al	Si	P	Ca	Notes
Spectrum 1	0.02	91.5	4.27	4.21	
Spectrum 2	N/D	98	0.36	1.64	
Spectrum 3	0.21	86.86	5.7	7.23	
Spectrum 4	2.39	34.17	19.98	43.46	
Spectrum 5	N/D	1.9	44.26	53.83	spot

Figure 76: Sample 12, magn x120. Table 27: Chemical analysis of the s12 areas outlined in fig. 36.

The pigment area seems to be confirmed by the analysis. However, in contrast to what has been previously stated of an underlying yellow stratum cannot be supported in this case. It is neither visually identifiable, nor is there any Fe detected to confirm this.

## 4. Discussion

The implementation of several different techniques required for complementary information seems to be necessary. A more complete picture on the technological aspects of these painted plaster fragments could be drawn with less inconclusive results.

All the pigments examined have been in the Bronze Age painter's palette and apart from the synthetic EB all the other colours are manufactured by naturally occurring sources. This means that specific minerals should be found in the painted layer. For two blue samples (s02, s07) the supposition was that the amphibole riebeckite was present while for s05 glaucophane. This use of riebeckite although rare in the mainland has been recorded in Mycenae, Thebes and Tyrins. The presence of glaucophane instead seems even more uncertain.

The samples with red, pink and yellow pigment were naturally considered to be made by earth ochres: hematite, goethite, limonite however these minerals could not be safely identified for each sample. The black pigments remained within the known and expected results of carbon black from plant or bone ash with probable impurities of Mn and Fe.

Lastly, for the grainy s06 the presence of Cl created the suspicion of the colour being a result of EB blue being degraded to phases of atacamite, paratacamite or clinoatacamite, which should be further investigated by examining solely the mortar.

Under these circumstances it is recommended that mineralogical microscopic examination with a polarising microscope should take place and X-ray diffraction analysis (XRD) to recognise the crystalline phases of minerals, their transformation and their composition. Relying solely on the XRD has its limitations especially in the recognition of amphiboles. Riebeckite and glaucophane (blue amphiboles) present similar main peak in XRD. Both have high Na<sub>2</sub>O content but a distinctive Fe/Mg ratio (Sotiropoulou et al, 2012), which is where the SEM analysis will become useful. Supplementary, a RAMAN spectroscopy analysis could safely confirm the SEM and XRF results regarding the blue pigments.

Furthermore, the PIXE-alpha technique could be employed as well. This one is characterised as surface-sensitive technique since its penetration depth varies between 5-



10 $\mu$ m and determines elementally the sample. It should be used complementary to the XRF because it is able to detect lighter elements (Z=11, Na) (Brecoulaki et al, 2008).

Another subject that has not been addressed at all is the matter of defining the painting technique (al fresco, secco or tempera).

The *fresco* technique is believed to have been used extensively in the BA Aegean. By that term is described the deposition of pigments on wet plaster that locks them in, through the creation of calcium carbonate (carbonisation of the lime). A list of parameters as to the identification of this technique includes the observation of the surface for fingernail impressions, fingerprints, string lines, paint brushes and initial drawings. (Brysaert, Perdikatsis, 2008) However, these are subject to personal interpretation. One perhaps argument in support of the *fresco* technique is the absence of filler that would quicken the drying procedure and harden the surface, rendering it unsuitable for applying the pigments. (Perdikatsis et al. 2000) The penetration of the pigment grains on the plaster cannot be a conclusive indicator. Yellow and red staining can be seen in greater depth since their pigment grains are smaller in size, while goethite and limonite are more soluble than hematite on the wet plaster. On the contrary, the grains of EB and amphiboles as larger are insoluble and therefore the relationship of grain size and solubility is an inverse one. (Perdikatsis et al. 2000) Of course, yellow and red penetrations occur in the *secco* technique as well due to osmotic pressures. The blue pigments though cannot be absorbed by a dry plaster. (Brysaert, Perdikatsis 2008) It should be noted though, that other factors can also affect the penetration depth such as the environmental conditions and the PH of the burial ground. (Perdikatsis et al. 2000) It is therefore quite difficult to distinguish which technique was used but it is a general agreement that both were, without being mutually exclusive.

The samples examined in cross section seemed to have quite distinct layers, with no significant penetration of the grains.

The technique known as *secco* describes painting on dried plaster with the help of a binder or medium. The medium is usually lime mixed with the pigments before their application on a dampened surface. Despite no distinction could be successfully made between primary and secondary calcite the use of lime as a binder cannot be rejected. It is also possible that an organic binder has been used as well. An analysis from the wall painting of an archer from Pylos by means of gas chromatography-mass spectrometry (GC-MS) and pyrolytic gas chromatography-mass spectrometry (PY/GC-MS) has revealed the use of an egg as a binder to the pigments. The simultaneous use of the techniques can identify proteins,

lipid materials (wax) or plant resins. (Brecoulaki et al, 2008). The samples were examined by means of GC/MS and resulted in proving both *secco* and *tempera* was used. In certain samples a mixture of binders was spotted. Each binder probably served a different purpose. For example, egg has stronger binding properties than tree/plant gums. The latter were seemingly used as an overcoat in order to protect the painted layer. Identification of glucose material in addition suggests that the purpose was to avoid brittleness. Finally, when animal glue is found in the mixture, it is considered as part of the preparation layer. In the samples examined several thick over-painted layers corroborate the use of the *secco* technique. (Brecoulaki et al. 2012a) The proximity of Iklaina to Pylos, the fact that it probably was an important center (because of its extent and all its architectural features) and the common techniques applied to wall paintings, makes the use of an organic media quite probable, but the case of the palace should not be representative of the whole region until more analyses are done.

## **5. Conclusion**



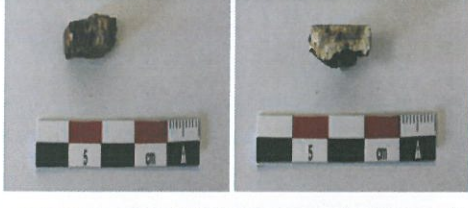










Overall, this study is only a basic work compared to all the information that can be extracted from these samples with the employment of more techniques and the right amount of experience on handling the material. It managed to provide a description and chemical analysis of the mortars and showed how they are related based on their composition.







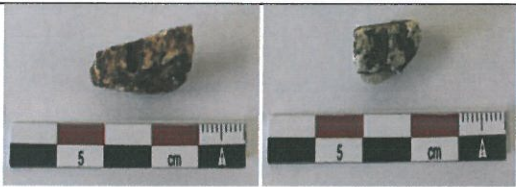

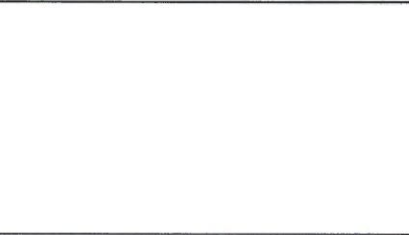





In regards with the pigments, almost the entire palette of the Bronze Age painter was confirmed after the examination. However, some compositional details remained inconclusive and require further research. More techniques should be employed so as to reach to safe results and further analyses to answer not only the mineralogical composition but also define the painting techniques and check for the possibility of organic binders.

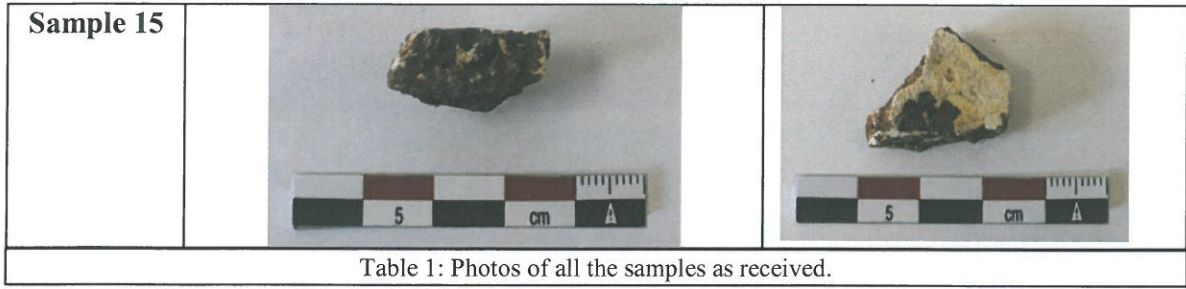


## Appendix

**Table 1.**

Sample number	Mortar side	Pigment side
Sample 01		
Sample 02		
Sample 03		
Sample 04		
Sample 05		
Sample 06		
Sample 07		

<b>Sample 08</b>		
<b>Sample 09</b>		
<b>Sample 10</b>		
<b>Sample 11</b>		
<b>Sample 12</b>		
<b>Sample 13</b>		
<b>Sample 14</b>		



**Table 2.**

	V	Cr	Mn	P	Co	Ni	Cu	Zn	As	Rb	Sr	Y	Zr	Nb	Mo	Sn	Sb	Ba	Pb	Th	U
1	0	33	215	0	46	0	0	9	5	0	12	12	7	1	122	4	39	66560	7	2	0
2	0	1	194	0	63	0	0	7	6	0	7	13	4	0	122	4	34	63144	6	2	0
2_cut	0	1	194	0	32	0	0	9	4	0	9	11	10	1	121	4	26	73615	7	2	0
3	0	3	324	0	2	8	15	14	5	6	117	16	22	2	27	3	18	9483	8	2	0
3_cut	0	3	324	0	4	23	32	20	4	7	132	19	30	3	22	3	16	9602	8	3	0
4	7	0	221	0	29	0	0	6	3	1	12	11	8	1	123	4	34	54470	7	2	2
5	0	0	169	0	60	0	0	5	4	0	7	13	6	0	121	4	31	72526	7	2	0
5_cut	0	0	169	0	7	13	33	22	5	11	100	31	19	3	31	3	25	11399	8	3	0
7	16	0	175	0	8	15	28	42	5	9	116	21	20	2	36	4	33	10378	9	2	0
7_cut	16	0	175	0	3	6	64	35	5	0	100	16	13	1	42	4	34	15523	10	2	0
8	39	114	896	0	63	0	0	4	3	0	12	10	13	1	122	4	38	64741	7	2	0
8_cut	39	114	896	0	3	5	80	30	4	5	89	16	11	1	43	4	42	17096	10	2	0
9	0	0	289	0	47	0	0	0	4	1	11	11	11	1	121	4	29	57699	7	2	0
9_cut	0	0	289	0	7	18	39	24	4	6	107	20	17	2	31	3	26	10777	9	3	0
10	7	0	307	0	4	16	28	13	4	2	85	21	23	2	26	3	13	9070	9	2	0
11	8	0	172	0	38	0	0	8	4	0	15	13	15	1	127	3	19	58124	7	2	0
11_cut	8	0	172	0	4	14	41	25	5	8	87	18	15	1	32	3	24	11137	8	2	0
12_cut	12	2	321	6206	3	24	42	21	4	2	109	16	25	2	28	3	23	10466	9	2	0
13	0	0	198	0	37	0	0	5	4	0	12	11	12	1	123	4	27	58790	7	2	0
14	0	0	238	0	34	0	0	7	3	0	13	12	12	1	122	3	25	55687	7	2	0
14_cut	0	0	238	0	9	27	24	39	4	7	115	21	29	2	25	3	16	9760	9	3	0
15_cut	0	3	202	0	4	13	77	18	4	0	64	19	18	2	37	3	24	14067	9	2	0

Table 2: Trace elements of mortars as detected in XRF. Values shown in ppm.

Table 3.


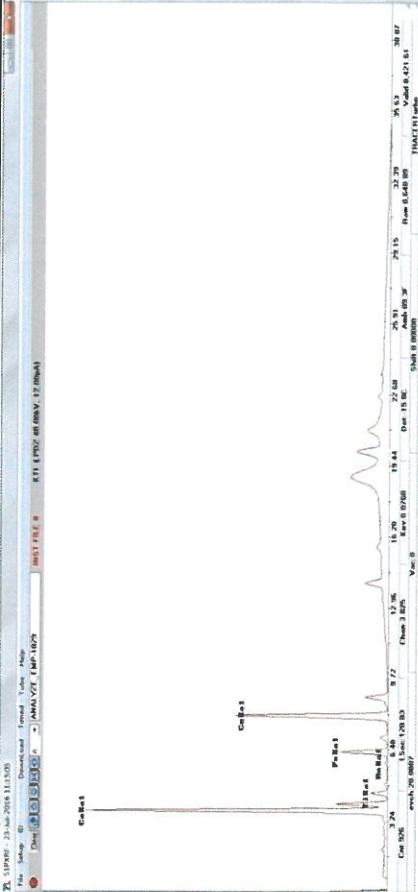
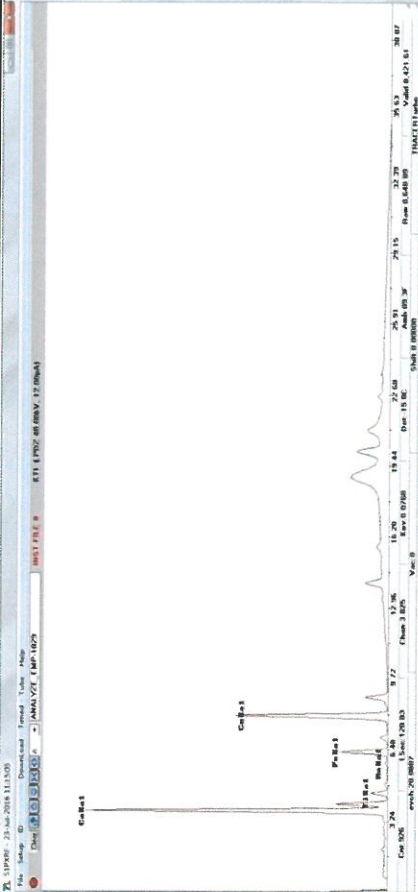
Sample 01																
				M	XRF	Na <sub>2</sub> O	MgO	Al <sub>2</sub> O <sub>3</sub>	SiO <sub>2</sub>	SO <sub>3</sub>	K <sub>2</sub> O	CaO	FeO	SUM		
O	SEM	Spectrum 1	1.434	0.792	12.637	38.177	0.585	1.413	44.963	0	100					
r		Spectrum 2			5.58	17.45		0	76.97	0	100					
t		Spectrum 3			4.79	23.97		2.02	64.03	5.19	100					
a	MEAN			1.15	3.87		0	94.97	0	100						
r	STDEV			3.84	15.0967		0.67333	78.6567	1.73							
s				2.36286	10.2546		1.16625	15.5388	2.99645							
Pigments																
		M	XRF	Na <sub>2</sub> O	MgO	Al <sub>2</sub> O <sub>3</sub>	SiO <sub>2</sub>	SO <sub>3</sub>	K <sub>2</sub> O	CaO	FeO	SUM				
O	SEM	Spectrum 1	4.91	33.18	1.52	56.44	2.07	1.87	100							
r		Spectrum 2	4.31	48.85	0.51	39.63	1.27	5.44	100							
t		Spectrum 3	4.79	41.23	0.8	44.53	1.46	7.19	100							
a	MEAN	4.67	41.0867	0.94333	46.8667	1.6	4.83333									
r	STDEV	0.3174902	7.83598	0.52003	8.64517	0.41797	2.71139									

Table 3: Complete results of mortar and pigment analysis of the samples in XRF and in SEM. Major element oxides in wt% normalised to 100% as detected in the XRF, analysis results in SEM are shown in compound %wt and are normalised.




Sample 02													
M o r t a r s	XRF	Na <sub>2</sub> O	MgO	Al <sub>2</sub> O <sub>3</sub>	SiO <sub>2</sub>	SO <sub>3</sub>	K <sub>2</sub> O	CaO	FeO	SUM			
		1.981	0.707	3.552	17.087	0.603	0.715	75.354	0	100			
	SEM	fresh_cut	1.981	0.707	3.552	17.087	0.603	0.715	75.354	0	100		
		Spectrum										Total	
		Spectrum 1										100	
		Spectrum 2										100	
		Spectrum 3										100	
		MEAN										99.77	
	STDEV										98.37		
													
P i g m e n t s	XRF	Na <sub>2</sub> O	MgO	Al <sub>2</sub> O <sub>3</sub>	SiO <sub>2</sub>	Cl	K <sub>2</sub> O	CaO	TiO <sub>2</sub>	MnO	FeO	Total	
		2.27	0.98	13.34	29.27	1.82	2.57	49.99	0.59	N/D	0.88	100	
	SEM	Spectrum 1 (blue)	2.67	1.67	18.43	39.66	0.15	2.5	31.37	0.19	N/D	3.53	100
		Spectrum 2 (blue)	1.36	2.67	19.57	50.61	1.23	3	15.57	0.87	N/D	5.52	100
		Spectrum 3 (blue)	2.1	1.77	17.12	39.85	1.07	2.69	32.31	0.55		3.31	
		MEAN	0.67	0.85	3.317	10.67	0.85	0.27	17.23	0.34		2.33	
		STDEV	1.9	0.85	24.8	52.16	0.93	3.53	7.76	0.17	0.26	7.64	100
		Spectrum 1 (red)	1.36	3.79	21.44	49.45	2.6	2.76	8.28	1.61	0.1	8.59	100
	Spectrum 2 (red)	3.32	1.12	20.8	49.43	2.27	2.67	10.7	0.31	0.03	9.36	100	
	Spectrum 3 (red)	2.19	1.92	22.35	50.35	1.93	2.99	8.91	0.7	0.13	8.53		
MEAN	1.01	1.63	2.15	1.57	0.88	0.47	1.57	0.79	0.12	0.86			
STDEV													
													

Table 3: Complete results of mortar and pigment analysis of the samples in XRF and in SEM. Major element oxides in wt% normalised to 100% as detected in the XRF, analysis results in SEM are shown in compound %wt and are normalised.




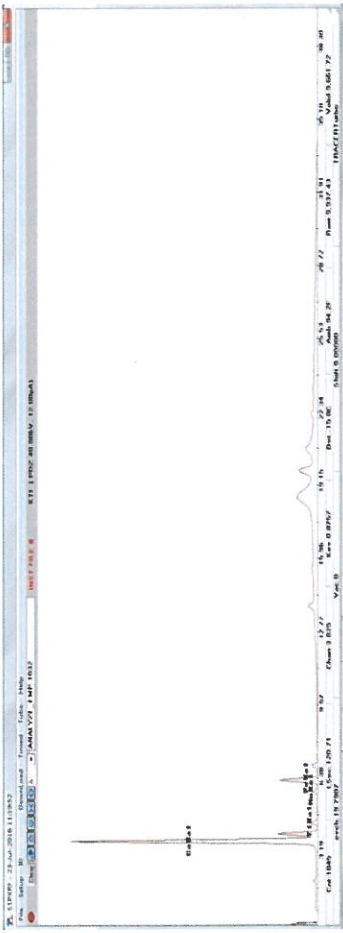
Sample 03		Mortars														
						XRF	Na <sub>2</sub> O	MgO	Al <sub>2</sub> O <sub>3</sub>	SiO <sub>2</sub>	SO <sub>3</sub>	K <sub>2</sub> O	CaO	FeO	SUM	
Pigments		XRF	fresh_cut	1.694	0.665	7.528	23.912	0.802	0.831	64.435	0.133	100				
			Spectrum	Al <sub>2</sub> O <sub>3</sub>	SiO <sub>2</sub>	CaO	Total									
			Spectrum 1	1.54	4.78	93.68	100									
			Spectrum 2	0.91	1.5	97.59	100									
			Spectrum 3	6.29	0	93.71	100									
			MEAN	2.913333	2.093333	94.993333	100									
STDEV	2.941196	2.444613	2.248829	100												
SEM		SEM	Spectrum	Na <sub>2</sub> O	Al <sub>2</sub> O <sub>3</sub>	SiO <sub>2</sub>	Cl	K <sub>2</sub> O	CaO	FeO	Total					
			Spectrum 1	3.19	10.44	19.04	2.27	1.93	58.55	4.58	100					
			Spectrum 2	2.2	12.89	32.2	2.13	2.32	45.44	2.82	100					
			Spectrum 3	1.96	15.14	30.36	1.3	2.68	43.54	5.02	100					
			MEAN	2.45	12.823333	27.2	1.9	2.31	49.17667	4.14	100					
			STDEV	0.65199693	2.350709	7.126402	0.524309	0.3751	8.172945	1.164131	100					

Table 3: Complete results of mortar and pigment analysis of the samples in XRF and in SEM. Major element oxides in wt% normalised to 100% as detected in the XRF, analysis results in SEM are shown in compound %wt and are normalised.

503

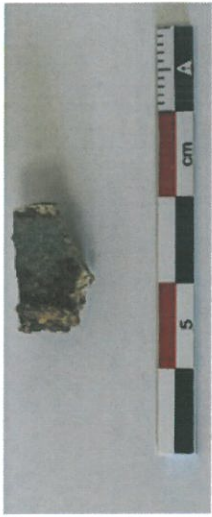
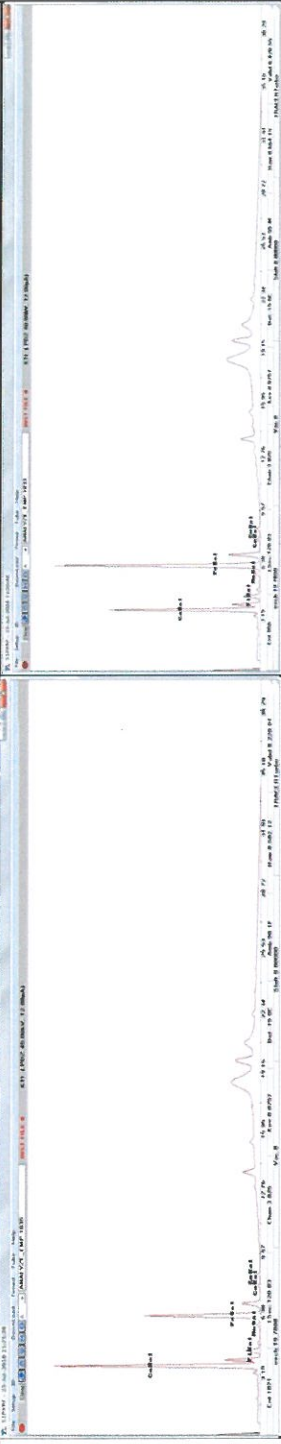
Sample 04											
M o r t a r s	XRF	Na <sub>2</sub> O	MgO	Al <sub>2</sub> O <sub>3</sub>	SiO <sub>2</sub>	SO <sub>3</sub>	K <sub>2</sub> O	CaO	FeO	SUM	
		2.279	1.099	0.740	10.823	0.547	0.474	84.038	0.000	100.000	
S E M	Spectrum			Al <sub>2</sub> O <sub>3</sub>	SiO <sub>2</sub>			CaO	FeO	Total	
	Spectrum 1			0.45	2.05			97.51	0	100	
	Spectrum 2			0.65	2.57			96.78	0	100	
	Spectrum 3			0.93	2.73			94.23	2.11	100	
	MEAN			0.676667	2.45			96.17333	0.703333		
STDEV			0.241109	0.355528			1.722101	1.218209			
P i g m e n t s	XRF										
	SEM	Na <sub>2</sub> O	MgO	Al <sub>2</sub> O <sub>3</sub>	SiO <sub>2</sub>	Cl	K <sub>2</sub> O	CaO	FeO	Total	
	Spectrum	4.55	1.66	19.94	43.97	2.44	3.23	21.94	2.28	100	
	Spectrum 1 (blue)	1.7	1.86	19.99	41.07	1.69	3.29	29.09	1.3	100	
	Spectrum 2 (blue)	6.29	2.46	21.37	44.4	1.12	4.06	19.02	0.27	100	
	MEAN	4.18	1.99	20.43	43.15	1.75	3.53	23.35	1.28		
	STDEV	2.32	0.42	0.81	1.81	0.66	0.46	5.18	1.01		
	Spectrum	Na <sub>2</sub> O	MgO	Al <sub>2</sub> O <sub>3</sub>	SiO <sub>2</sub>	Cl	K <sub>2</sub> O	CaO	FeO	Total	
	Spectrum 1 (black)	3.53	3.19	22.42	54.88	2.98	3.67	8.79	0.55	100	
	Spectrum 2 (black)	1.21	3.34	18.9	51.14	0.99	3.8	12.65	7.97	100	
	Spectrum 3 (black)	0.1	3.62	21.1	59.77	0.73	1.75	7.53	5.39	100	
	MEAN	1.61	3.38	20.81	55.26	1.57	3.073	9.66	4.64		
	STDEV	1.75	0.22	1.78	4.33	1.23	1.15	2.67	3.77		

Table 3: Complete results of mortar and pigment analysis of the samples in XRF and in SEM. Major element oxides in wt% normalised to 100% as detected in the XRF, analysis results in SEM are shown in compound %wt and are normalised.

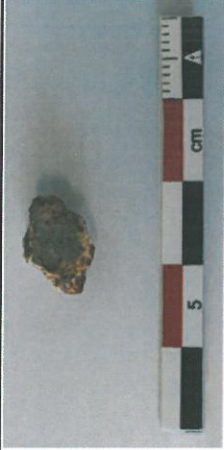
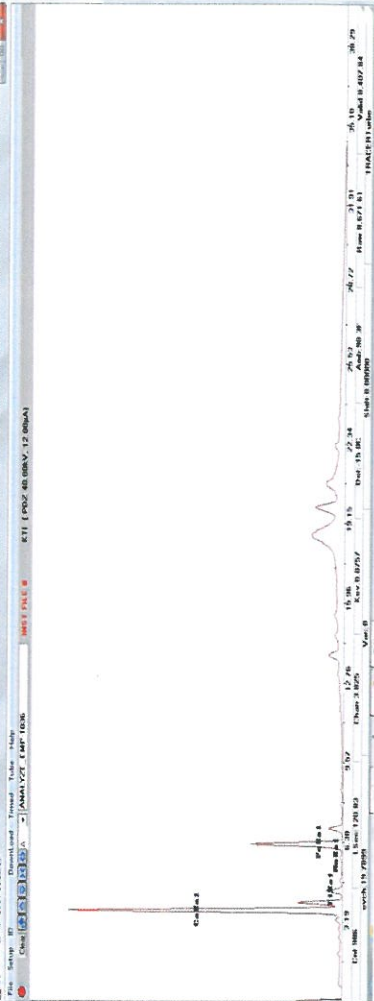
Sample 05													
M o r t a r s	XRF	Na <sub>2</sub> O	Al <sub>2</sub> O <sub>3</sub>	MgO	SiO <sub>2</sub>	SO <sub>3</sub>	K <sub>2</sub> O	CaO	FeO	SUM			
		fresh_cut	2.118	5.624	19.423	1.606	0.705	68.904	0	100			
	SEM	Spectrum	2.071	5.5	1.584	18.993	1.57	0.689	67.378	2.214	100		
		Spectrum 1	Al <sub>2</sub> O <sub>3</sub>										
		Spectrum 2	1.99	7.55									
		Spectrum 3	0	0									
		MEAN	1.1	4.7									
		STDEV	1.03	4.083333									
	P i g m e n t s	XRF	0.996845	3.812589	CaO								
			90.46	100									
100			94.21										
94.89			4.806215										
													
Spectrum			Na <sub>2</sub> O	Al <sub>2</sub> O <sub>3</sub>	SiO <sub>2</sub>	Cl	K <sub>2</sub> O	CaO	FeO	CuO	Total		
Spectrum 1			2.64	13.1	26.58	1.47	2.15	49.31	4.45	0.31	100		
Spectrum 2			5.07	13.83	29.45	2.11	1.86	43.91	3.77	0	100		
Spectrum 3			1.93	23.12	50.02	2.12	3.3	15.84	3.67	0	100		
MEAN			3.21	16.68	35.35	1.9	2.44	36.35	3.96				
STDEV	1.65	5.59	12.79	0.37	0.76	17.97	0.42						

Table 3: Complete results of mortar and pigment analysis of the samples in XRF and in SEM. Major element oxides in wt% normalised to 100% as detected in the XRF, analysis results in SEM are shown in compound %wt and are normalised.

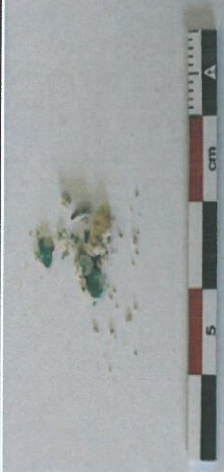
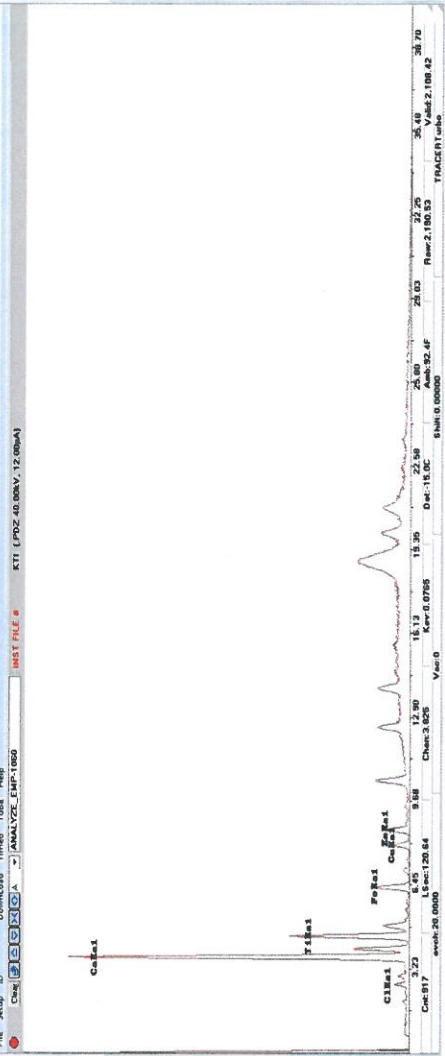
Sample 06	SEM										
		M	MgO	Al <sub>2</sub> O <sub>3</sub>	SiO <sub>2</sub>	CaO	FeO	Total			
Pigments	Spectrum 1	2.16	1.49	9.85	85.03	1.47	100				
	Spectrum 2	2.17	1.54	4.17	90.27	1.86	100				
	Spectrum 3	3.77	0.92	8.12	87.2	0	100				
	MEAN	2.7	1.316667	7.38	87.5	1.11					
	STDEV	0.92666067	0.344432	2.911409	2.63285	0.980867					
											
SEM	Spectrum	MgO	Al <sub>2</sub> O <sub>3</sub>	SiO <sub>2</sub>	SO <sub>3</sub>	Cl	CaO	TiO <sub>2</sub>	FeO	Total	
	Spectrum 1	5.84	12.76	22.68	6.94	2.62	37.34	8.48	3.33	100	
	Spectrum 2	3.96	9.76	27.05	2.66	1.31	38.84	11.94	4.47	100	
	Spectrum 3	3.52	10.07	27.37	8.04	2.68	40.92	5.91	1.48	100	
	MEAN	4.44	10.86	25.7	5.88	2.2	39.03	8.78	3.093		
	STDEV	1.23	1.65	2.62	2.84	0.77	1.8	3.03	1.51		

Table 3: Complete results of mortar and pigment analysis of the samples in XRF and in SEM. Major element oxides in wt% normalised to 100% as detected in the XRF, analysis results in SEM are shown in compound %wt and are normalised.


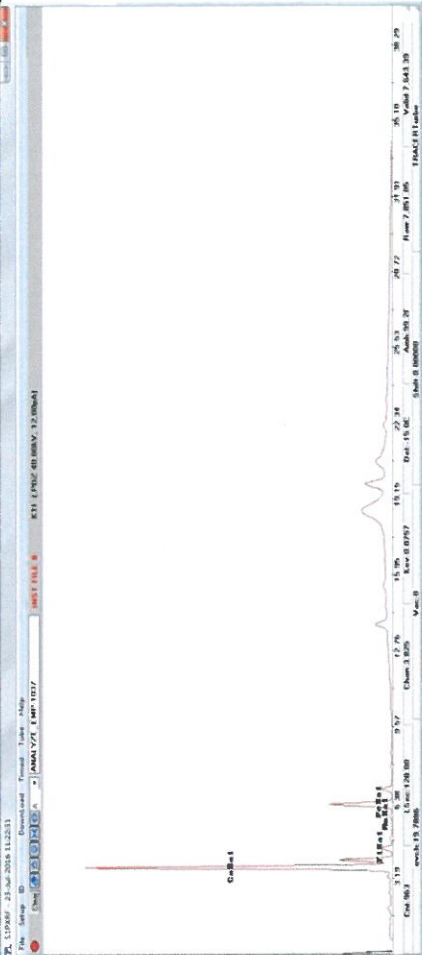
Sample 07													
M o r t a r s	XRF	Na <sub>2</sub> O	MgO	Al <sub>2</sub> O <sub>3</sub>	SiO <sub>2</sub>	SO <sub>3</sub>	K <sub>2</sub> O	CaO	FeO	SUM			
		2.226	2.435	2.107	14.185	1.14	0.474	74.554	2.879	100			
		fresh_cut	2.258	2.137	14.388	1.156	0.481	75.623	1.486	100			
		Spectrum		Al <sub>2</sub> O <sub>3</sub>	SiO <sub>2</sub>	Cl	CaO				Total		
		Spectrum 1		0.38	1.7	0	97.92			100			
	Spectrum 2		0.5	1.47	0	98.03			100				
	Spectrum 3		1.81	0.9	1.57	95.72			100				
	MEAN		0.896667	1.356667	0.523333	97.22333							
	STDEV		0.793242	0.411866	0.90644	1.303086							
	P i g m e n t s	XRF	Na <sub>2</sub> O	MgO	Al <sub>2</sub> O <sub>3</sub>	SiO <sub>2</sub>	Cl	K <sub>2</sub> O	CaO	FeO	SUM		
2.69			3.2	22.48	45.04	2.74	2.78	18.55	2.5	100			
Spectrum 1			4.22	0.75	24.13	46.17	1.88	2.25	17.95	2.64	100		
Spectrum 2			3.6	1.32	21.31	37.96	1.61	2.46	27.66	4.07	100		
Spectrum 3			3.503333333	1.756667	22.64	43.05667	2.076667	2.496667	21.38667	3.07	100		
MEAN		0.76956698	1.282043	1.416792	4.449858	0.590113	0.266896	5.441143	0.86885				
STDEV													
													

Table 3: Complete results of mortar and pigment analysis of the samples in XRF and in SEM. Major element oxides in wt% normalised to 100% as detected in the XRF, analysis results in SEM are shown in compound %wt and are normalised.

[8A]

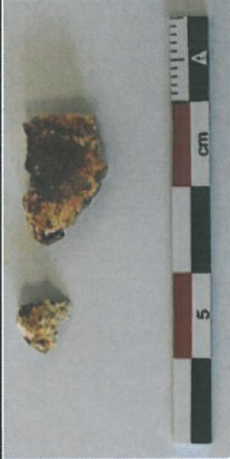
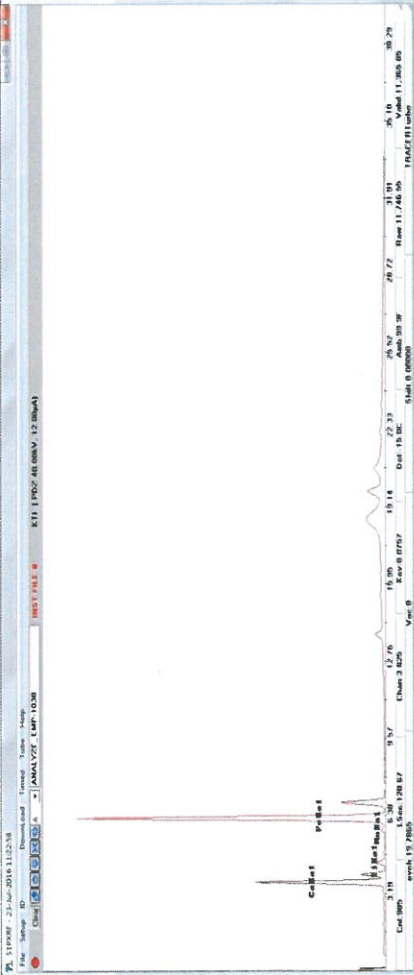
Sample 08												
M o r t a r s	XRF	Na <sub>2</sub> O	MgO	Al <sub>2</sub> O <sub>3</sub>	SiO <sub>2</sub>	SO <sub>3</sub>	K <sub>2</sub> O	CaO	FeO	SUM		
		1.86	2.601	2.989	12.869	1.204	0.291	78.186	0	100		
	SEM	fresh_cut	1.846	2.58	2.966	12.768	1.195	0.288	77.571	0.787	100	
		Spectrum	Al <sub>2</sub> O <sub>3</sub>		SiO <sub>2</sub>		CaO				Total	
		Spectrum 1	2.65		2.92		94.43				100	
		Spectrum 2	0		1.91		98.09				100	
		Spectrum 3	2.27		2.45		95.27				100	
	MEAN	1.64		2.426667		95.93						
	STDEV	1.432934		0.505404		1.917185						
	P i g m e n t s	XRF										
Na <sub>2</sub> O			MgO	Al <sub>2</sub> O <sub>3</sub>	SiO <sub>2</sub>	Cl	K <sub>2</sub> O	CaO	FeO	Total		
1.85		0.95	25.93	53.5	1.24	2.88	4.94	8.71	100			
SEM		Spectrum 1	2.89	1.49	25.01	56.17	1.62	1.92	5.24	5.66	100	
		Spectrum 2	4.15	2.1	22.38	50.59	2.01	1.52	15.94	1.31	100	
		Spectrum 3	2.96333333	1.513333	24.44	53.42	1.623333	2.106667	8.706667	5.226667		
		MEAN	1.15175229	0.575355	1.842363	2.79086	0.385011	0.698952	6.266046	3.718983		
		STDEV										

Table 3: Complete results of mortar and pigment analysis of the samples in XRF and in SEM. Major element oxides in wt% normalised to 100% as detected in the XRF, analysis results in SEM are shown in compound %wt and are normalised.

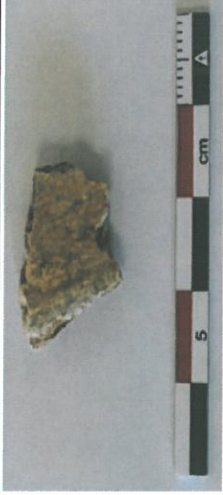
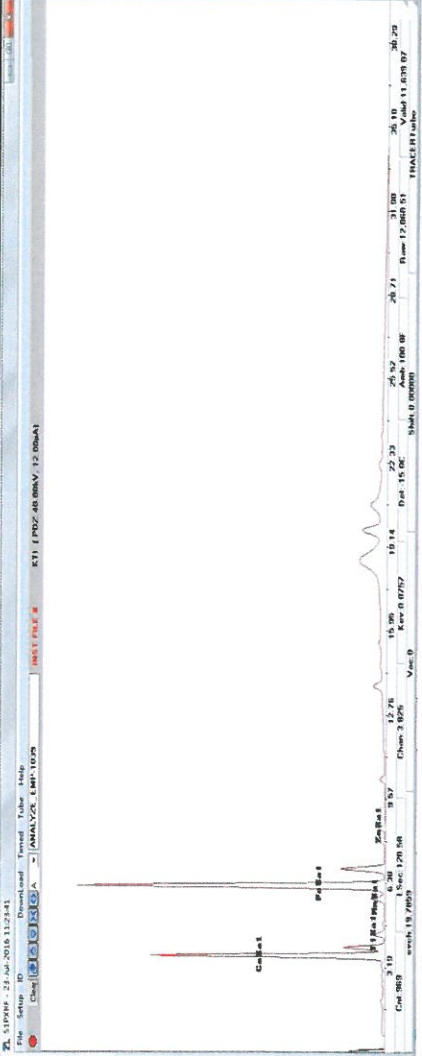
Sample 09		Mortars															
						XRF	Na <sub>2</sub> O	MgO	Al <sub>2</sub> O <sub>3</sub>	SiO <sub>2</sub>	SO <sub>3</sub>	K <sub>2</sub> O	CaO	FeO	SUM		
Pigments		SEM	fresh_cut	2.198	1.079	5.91	19.789	0.769	0.599	69.656	0	100					
			Spectrum	Al <sub>2</sub> O <sub>3</sub>	SiO <sub>2</sub>	CaO	MnO	FeO	Total								
			Spectrum 1	5.02	9.16	1.25	78.08	0	6.5	100							
			Spectrum 2	2.09	9.11	0	85.82	0	2.98	100							
			Spectrum 3	4.39	8.59	0	83.52	3.5	0	100							
		MEAN	3.833333	8.953333	0.416667	82.47333	1.166667	3.16									
		STDEV	1.542282	0.315647	0.721688	3.974737	2.020726	3.253736									
Pigments		SEM	Spectrum	Al <sub>2</sub> O <sub>3</sub>	SiO <sub>2</sub>	CaO	FeO	Total									
			Spectrum 1	5.93	11.62	67.03	15.42	100									
			Spectrum 2	8.34	18.21	53.75	19.7	100									
			Spectrum 3	4.68	15.58	54.4	25.35	100									
			MEAN	6.31666667	15.13667	58.39333	20.15667										
		STDEV	1.86038526	3.317293	7.48663	4.980726											

Table 3: Complete results of mortar and pigment analysis of the samples in XRF and in SEM. Major element oxides in wt% normalised to 100% as detected in the XRF, analysis results in SEM are shown in compound %wt and are normalised.

667

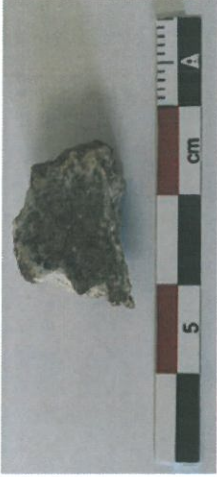
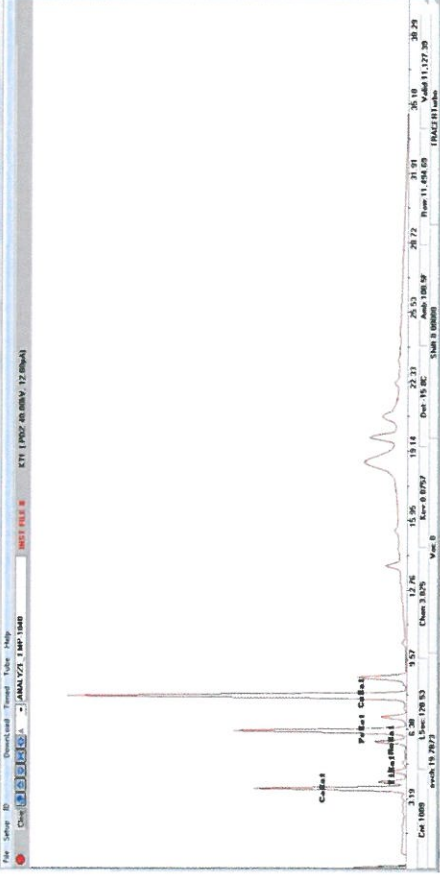
Sample 10													
M o r t a r s	XRF	Na <sub>2</sub> O	MgO	Al <sub>2</sub> O <sub>3</sub>	SiO <sub>2</sub>	SO <sub>3</sub>	K <sub>2</sub> O	CaO	FeO	SUM			
		2.254	0.829	0.666	11.535	0.474	0.406	83.835	0	100			
	SEM	Spectrum	MgO	Al <sub>2</sub> O <sub>3</sub>	SiO <sub>2</sub>			CaO					
		Spectrum 1	0.42	2.73	16.82			80.03					
		Spectrum 2	0	4.38	6.14			89.48					
		Spectrum 3	0	9.38	0			90.62					
		MEAN	0.14	5.496667	7.653333			86.71					
STDEV	0.242487	3.462778	8.511506			5.813063							
P i g m e n t s	XRF												
		Spectrum	Al <sub>2</sub> O <sub>3</sub>	K <sub>2</sub> O	CaO	FeO	CuO	Total					
		Spectrum 1	3.04	0.54	49.05	2.04	6.01	100					
		Spectrum 2	8	1.76	26.63	5.71	1.99	100					
		Spectrum 3	1.37	0.16	56.67	1.43	3.72	100					
		MEAN	4.14	0.82	44.12	3.06	3.9						
		STDEV	3.49	0.84	15.61	2.31	2.02						

Table 3: Complete results of mortar and pigment analysis of the samples in XRF and in SEM. Major element oxides in wt% normalised to 100% as detected in the XRF, analysis results in SEM are shown in compound %wt and are normalised.




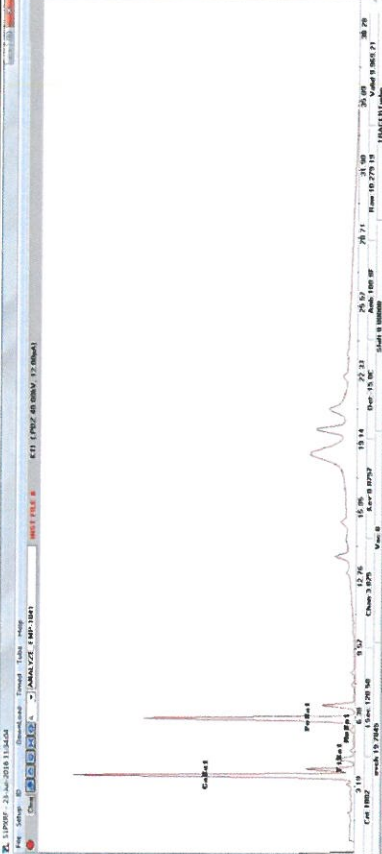
Sample 11												
M o r t a r s	XRF	Na <sub>2</sub> O	MgO	Al <sub>2</sub> O <sub>3</sub>	SiO <sub>2</sub>	SO <sub>3</sub>	K <sub>2</sub> O	CaO	FeO	SUM		
		fresh_cut	1.93	0.591	1.682	11.936	0.892	0.496	82.473	0	100	
	SEM	Spectrum	1.899	0.582	1.655	11.742	0.878	0.488	81.138	1.619	100	Total
		Spectrum 1				Si			Ca		100	100
		Spectrum 2				0			100		87.68	100
		Spectrum 3				12.32			100		100	100
		MEAN				4.106667			95.89333		100	100
STDEV				7.112955			7.112955					
P i g m e n t s	XRF											
		Spectrum	Al <sub>2</sub> O <sub>3</sub>	K <sub>2</sub> O	SiO <sub>2</sub>	CaO	FeO	CuO	Total			
	Spectrum 1	7.65	1.52	17.29	72.18	1.16	0.2	100				
	Spectrum 2	17.36	3.51	48.87	28	2.86	0	100				
	Spectrum 3	16.46	2.02	37.8	37.38	5.35	0.99	100				
	MEAN	13.82	2.35	34.65	45.85	3.12	0.59					
	STDEV	5.37	1.04	16.023	23.27	2.11	0.56					

Table 3: Complete results of mortar and pigment analysis of the samples in XRF and in SEM. Major element oxides in wt% normalised to 100% as detected in the XRF, analysis results in SEM are shown in compound %wt and are normalised.

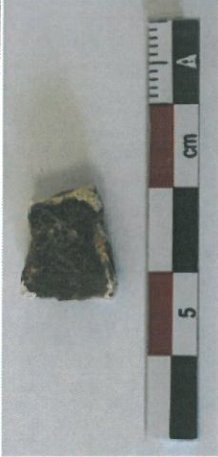

Sample 12													
M o r t a r s	XRF	fresh_cut	Na <sub>2</sub> O	MgO	Al <sub>2</sub> O <sub>3</sub>	SiO <sub>2</sub>	SO <sub>3</sub>	K <sub>2</sub> O	CaO	FeO	SUM		
		Spectrum 1	1.658	0.908	0	13.08	0	0.47	83.884	0	100		
	SEM	Spectrum 2			Al <sub>2</sub> O <sub>3</sub>	SiO <sub>2</sub>	P	K <sub>2</sub> O	CaO			Total	
		Spectrum 3			0.21	0.48	1.19	0.06	98.05			100	
		MEAN			2.66	4.72	0	0.64	91.98			100	
		STDEV			1.77	2.42	2.13	0	93.68			100	
					1.546667	2.54	1.106667	0.233333	94.57				
			1.240175	2.122546	1.067442	0.353459	3.131342						
P i g m e n t s	XRF												
		Spectrum 1	Al <sub>2</sub> O <sub>3</sub>	SiO <sub>2</sub>	P	K <sub>2</sub> O	CaO	MnO	FeO	Total			
		Spectrum 2	14.09	32.47	15.17	2.89	22.63	5.13	7.61	100			
		Spectrum 3	18.12	39.63	9.76	3.67	14	8.27	6.57	100			
		MEAN	18.7	42.12	9.06	3.88	12.53	4.46	9.25	100			
		STDEV	16.97	38.0733333	11.33	3.48	16.38667	5.953333	7.81				
			2.510955993	5.00979374	3.343905	0.521632	5.456614	2.034068	1.351148				

Table 3: Complete results of mortar and pigment analysis of the samples in XRF and in SEM. Major element oxides in wt% normalised to 100% as detected in the XRF, analysis results in SEM are shown in compound %wt and are normalised.

[67]


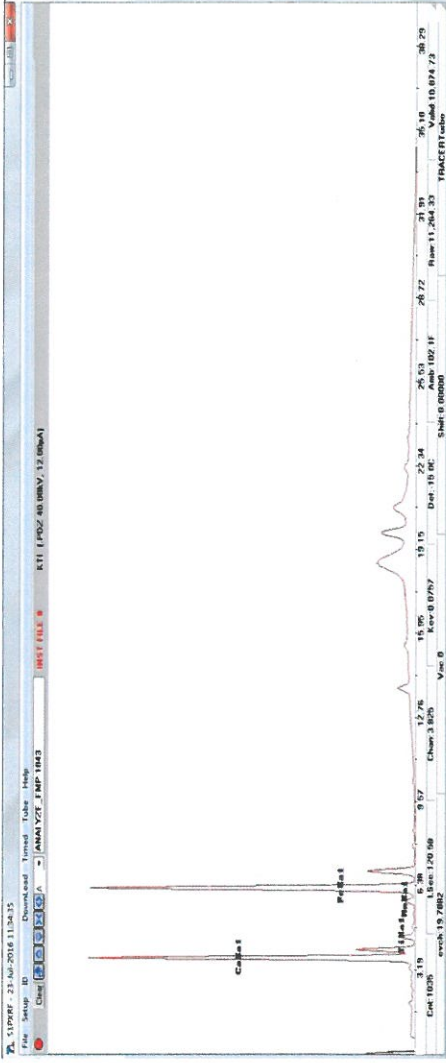
Sample 13											
M o r t a r s	XRF	Na <sub>2</sub> O	MgO	Al <sub>2</sub> O <sub>3</sub>	SiO <sub>2</sub>	SO <sub>3</sub>	K <sub>2</sub> O	CaO	FeO	SUM	
		2.13	1.062	2.47	14.905	0.963	0.562	77.908	0	100	
	SEM	Spectrum	Al <sub>2</sub> O <sub>3</sub>		SiO <sub>2</sub>		CaO		FeO		Total
		Spectrum 1	2.02		4.94		93.04				100
		Spectrum 2	0.48		4.54		94.99				100
		Spectrum 3	1.38		1.83		96.78				100
		MEAN	1.293333		3.77		94.93667				100
STDEV	0.773649		1.691952		1.87057						
P i g m e n t s	XRF										
		Al <sub>2</sub> O <sub>3</sub>	K <sub>2</sub> O	CaO	FeO	Total					
	Spectrum	16.66	38.65	29.06	14.23	100					
	Spectrum 1	16.25	34.69	34.28	13.22	100					
	Spectrum 2	13.21	30.42	35.5	19.95	100					
	MEAN	15.373333	34.58667	32.94667	15.8						
	STDEV	1.88468388	4.115973	3.42078	3.629311						

Table 3: Complete results of mortar and pigment analysis of the samples in XRF and in SEM. Major element oxides in wt% normalised to 100% as detected in the XRF, analysis results in SEM are shown in compound %wt and are normalised.

Sample 14																		
M o r t a r s	XRF	Na <sub>2</sub> O	MgO	Al <sub>2</sub> O <sub>3</sub>	SiO <sub>2</sub>	SO <sub>3</sub>	K <sub>2</sub> O	CaO	FeO	SUM								
		fresh_cut	1.613	0.659	2.784	13.557	0.63	0.537	80.22	0	100							
	SEM	Spectrum	1.596	0.652	2.755	13.419	0.623	0.532	79.405	1.017	100							
		Spectrum 1			Al <sub>2</sub> O <sub>3</sub>	SiO <sub>2</sub>			CaO			100						
		Spectrum 2			0.71	3.95			95.34			100						
		Spectrum 3			1.19	1.85			96.96			100						
		MEAN			0.41	3.63			95.95			100						
	STDEV			0.77	3.143333			96.08333			100							
	P i g m e n t s	XRF	Na <sub>2</sub> O	MgO	Al <sub>2</sub> O <sub>3</sub>	SiO <sub>2</sub>	Cl	K <sub>2</sub> O	CaO	FeO	Total							
			Spectrum	4.23	3.8	24.06	53.13	2.05	2.44	7.26	3.04	100						
SEM		Spectrum 1	3.16	2.52	22.53	57.86	0.78	3.11	5.9	4.14	100							
		Spectrum 2	4.47	1.94	28.46	49.91	2.55	3.4	8.7	0.57	100							
		MEAN	3.95333333	2.753333	25.01667	53.63333	1.793333	2.983333	7.286667	2.583333	100							
		STDEV	0.69744773	0.9517	3.078577	3.998829	0.912487	0.492375	1.40019	1.828287	100							

Table 3: Complete results of mortar and pigment analysis of the samples in XRF and in SEM. Major element oxides in wt% normalised to 100% as detected in the XRF, analysis results in SEM are shown in compound %wt and are normalised.

[69]


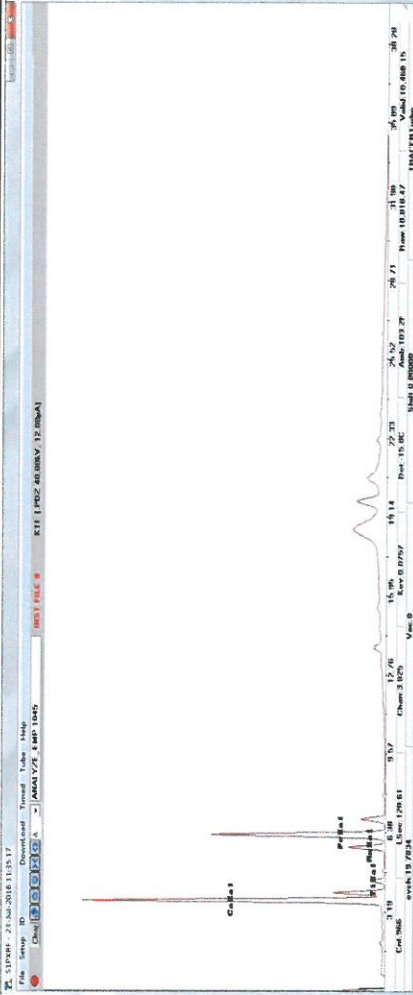
Sample 15													
M o r t a r s	XRF	fresh_cut	Na <sub>2</sub> O	MgO	Al <sub>2</sub> O <sub>3</sub>	SiO <sub>2</sub>	SO <sub>3</sub>	K <sub>2</sub> O	CaO	FeO	SUM		
		Spectrum	1.961	0.636	2.107	13.962	0.669	0.534	79.223	0.908	100		
	SEM	Spectrum 1			Al <sub>2</sub> O <sub>3</sub>	SiO <sub>2</sub>						Total	
		Spectrum 2			0.69	2.6						100	
		Spectrum 3			0.53	2.3						100	
		MEAN			1.07	1.21						100	
		STDEV			0.763333	2.036667						97.19667	
					0.277369	0.73146						0.510523	
	P i g m e n t s	XRF		Al <sub>2</sub> O <sub>3</sub>	SiO <sub>2</sub>	Cl	K <sub>2</sub> O	CaO	MnO	FeO	Total		
			Spectrum 1	13.04	52.28	1.34	1.93	5.66	1.12	24.62	100		
Spectrum 2		15.04	45.66	1.63	2.12	19.39	4.81	11.35	100				
Spectrum 3		14.54	47.7	1.04	1.47	16.23	4.45	14.56	100				
MEAN		14.2066667	48.54667	1.336667	1.84	13.76	3.46	16.84333					
STDEV		1.040833	3.390241	0.295014	0.334215	7.190542	2.034478	6.923398					
													

Table 3: Complete results of mortar and pigment analysis of the samples in XRF and in SEM. Major element oxides in wt% normalised to 100% as detected in the XRF, analysis results in SEM are shown in compound %wt and are normalised.

## References

1. Brecoulaki H., Fiorin E., Vigato P.A., (2006) The funerary klinai of tomb 1 from Amphipolis and a sarcophagus from ancient Tragilos, eastern Macedonia: a physico-chemical investigation on the painting materials, *Journal of Cultural Heritage*, 7, p. 301-311.
2. Brecoulaki H., (2008) An archer from the palace of Nestor, a new wall-painting fragment in the Chora museum, *Hesperia*, 77, p. 363-397.
3. Brecoulaki H., Andreotti A., Bonaduce I., Colombini M. P., Lluveras A. (2012a) "Characterization of organic media in the wall-paintings of the "Palace of Nestor" at Pylos, Greece: evidence for a secco painting techniques in the Bronze Age", *JASC*, 39, 9, September 2012, p. 2866-2876.
4. Brysbaert, A., V. Perdikatsis. (2008) 'Bronze Age Painted Plaster from the Greek Mainland: A Comparative Study of its Technology by Means of XRD Analysis and Optical Microscopy Techniques'. Paper presented at Proceedings of the 4th Symposium of the Hellenic Society for Archaeometry. National Hellenic Research Foundation, Athens, 28-31 May 2003. England, Oxford: BAR International Series 1746, p. 421-429.
5. Brysbaert, Ann. (2008) *The power of technology in the Bronze Age eastern Mediterranean: the case of the painted plaster*. London; Oakville, CT: Equinox Publications.
6. Cosmopoulos, M. B. (2012) Ανασκαφή Ίκλαινας Μεσσηνίας, in: *Πρακτικά της εν Αθήναις Αρχαιολογικής εταιρείας του έτους 2009*, Αθήνα, p. 99-118.
7. Cosmopoulos, M. B. (2013) Ανασκαφή Ίκλαινας Μεσσηνίας, in: *Πρακτικά της εν Αθήναις Αρχαιολογικής εταιρείας του έτους 2010*, Αθήνα, p. 33-51.
8. Cosmopoulos, M. B. (2015a) A Group of New Mycenaean Frescoes from Iklaina, Pylos in: Brecoulaki, H., Davis, J. L., Stoker, S. R. (eds.) *Mycenaean Wall Painting in Context, New Discoveries, Old Finds Reconsidered*. ΜΕΛΕΤΗΜΑΤΑ, 72, National Hellenic Research Foundation, Institute of Historical Studies, p. 249-259.
9. Cosmopoulos, M. B. (2015b) Ανασκαφή Ίκλαινας Μεσσηνίας, in: *Πρακτικά της εν Αθήναις Αρχαιολογικής εταιρείας του έτους 2013*, Αθήνα, p. 51-55.
10. Eastaugh, N., Walsh, V., Chaplin, T., Siddall. R. (2004) *The Pigment Compendium, a dictionary of historical pigments*, Oxford: Elsevier.

11. Filippakis, S., E., Perdikatsis, B., Paradellis, T. (1976) An Analysis of Blue Pigments from the Greek Bronze Age, *Studies in Conservation*, 21. Maney Publishing, International Institute for Conservation of Historic and Artistic Works, p. 143–153.
12. Gimenez, J. (2015) Finding hidden chemistry in ancient Egyptian artifacts: pigment degradation taught in a chemical engineering course, *Journal of Chemical Education*, 92, pp. 456-462.
13. Liritzis I, Zacharias N. (2010), Portable XRF for Use in Archaeology, in S. Shackley (ed.) *XRF Technology and Modern Applications*, New York: Springer-Verlag.
14. Moropoulou, N. Zacharias, E.T. Delegou, B. Maróti, Zs. Kasztovszky (2016) Analytical and technological examination of glass tesserae from Hagia Sophia, *Microchemical Journal*, 126, p. 170-184.
15. Morgan, Lyvia, ed. (2005) *Aegean Wall Painting: a Tribute to Mark Cameron*. London: British School at Athens.
16. Perdikatsis, B. (1993) 'Analysis of Pigments from ancient Greek art monuments.' Paper presented at the Proceedings of the scientific symposium 'Art and Technology', Athens p.271-279.
17. Perdikatsis, V. (1998) 'Analysis of Greek Bronze Age wall painting Pigments'. Paper presented at the Centro Universatio Europeo per Beni Culturali, «La couleur dans la peinture et l'emailage de l'Egypte ancienne: actes de la table Ronde», Ravello, 20-22 March 1997. Bari: Edipuglia, p.103-108.
18. Perdikatsis V., V. Kilikoglou, S. Sotiropoulou, E. Chryssikopoulou. (2000) 'Physicochemical characterisation of pigments from Thera wall paintings'. Paper presented at Proceedings of the first International Symposium: The wall paintings of Thera. (1), Athens: Thera Foundation, p.103-129.
19. Profi, S., L. Weier, and S. E. Filippakis. (1974) "X-ray Analysis of Greek Bronze Age Pigments from Mycenae". *Studies in Conservation* 19 (2). Maney Publishing, International Institute for Conservation of Historic and Artistic Works, p. 105–112.
20. Profi, S., L. Weier, and S. E. Filippakis. (1976) "X-ray Analysis of Greek Bronze Age Pigments from Knossos". *Studies in Conservation* 21 (1). Maney Publishing, International Institute for Conservation of Historic and Artistic Works, p. 34–39.
21. Profi, S., B. Perdikatsis, and S. E. Filippakis. (1977) "X-ray Analysis of Greek Bronze Age Pigments from Thera (Santorini)". *Studies in Conservation* 22 (3). Maney

- Publishing, International Institute for Conservation of Historic and Artistic Works, p. 107–115.
22. Schiegl, S., Weiner, K.L., El Goresy, A. (1989) Discovery of copper chloride cancer in ancient Egyptian polychromic wall paintings and faience: a developing archaeological disaster. *Naturwissenschaften*, 76, pp. 393-400.
  23. Sotiropoulou, S., Perdikatsis, V., Birtacha, K., Apostolaki, C., Devetzi, A. (2012) Physicochemical characterisation and provenance of clouring materians from Akrotiti-Thera in relation to their archaeological context and application, Springer-Verlag, *Archaeol Anthropol Sci*, DOI 10.1007/s12520-012-0099-y
  24. Μαρινάτος, Σ. Ν. (1954) Ανασκαφαί εν Πύλω in *Πρακτικά της Εν Αθήναις Αρχαιολογικής Εταιρείας (Prakt)*, T. 109, p. 299-316.